Desalination and Water Treatment
www.deswater.com

doi: 10.5004/dwt.2020.25083

184 (2020) 94–129
April

Progress of fitting models describing transport phenomena within nanofiltration membranes: a review

Bouchareb Abderrezak[a], Metaiche Mehdi[a], Nadjib Drouiche[b,*], I. Gede Wenten[c], Lounici Hakim[d]

[a]*Laboratory of Energy, Water Environment, PM3E, Bouira University, Algeria, emails: a.bouchareb@univ-bouira.dz (B. Abderrezak), metiche022000@yahoo.fr (M. Mehdi)*
[b]*Department of Environmental Engineering, Technology of Semi-conductor for the Energetic Research Center (CRTSE), Algiers, Algeria, email: nadjibdrouiche@yahoo.fr (N. Drouiche)*
[c]*Department of Chemical Engineering, Institut Teknologi Bandung, JI. Ganesha 10, Bandung 40132, Indonesia, email: igw@che.itb.ac.id (I. Gede Wenten)*
[d]*Laboratory of Materials and Sustainable Development, Bouira University, Algeria, email: hakim_lounici@yahoo.ca (L. Hakim)*

Received 26 May 2019; Accepted 25 October 2019

ABSTRACT

Nanofiltration membranes have been widely used in various separation and purification applications such as industrial wastewater treatment, food, and pharmaceutical industries. During the last three decades, several mathematical models have been progressing to illustrate the transport phenomena and both the expression of water and solute fluxes in such a process. This paper looks into the aims and the limitations of the most used models by the research community, which gives a better understanding of these phenomena according to the complexity of this process. In this review, 24 mathematical models were presented from (Solution–diffusion models, irreversible thermodynamics models, extended Nernst–Planck equation and the Maxwell–Stefan model) those who give an overview contribution in this such study regarding the frequently problems (multi-ions solution, charged/uncharged solutes, pore geometry, membrane charge, and concentration polarization), each model present in this review was discussed in the terms of assumptions, advantages and disadvantages noticed.

Keywords: Nanofiltration; Mathematical models; Solution–diffusion models; Irreversible thermodynamic models; Extended Nernst–Planck models

1. Introduction

Nanofiltration is a pressure-driven membrane process, that able to remove divalent ions as well as multivalent ions from a solution. Nanofiltration membrane is considered to be “leaky” reverse osmosis (RO) membrane because of its similarity to RO, the exception is that nanofiltration membranes allow more ions to pass through than RO membranes in which it needs lower operating pressure than RO case. In general, nanofiltration has two distinct properties [1–3]:

- Nanofiltration has molecular weight cut off (MWCO) between MWCO of RO and ultrafiltration membranes approximately 300–500 g/mol [1,2]. This MWCO value corresponds to the membrane pore size.
- Nanofiltration membranes have a slightly charged surface. The charge interaction plays a dominant role when

---

[*] Corresponding author.

1944-3994/1944-3986 © 2020 Desalination Publications. All rights reserved.

the dimensions of the pores are less than one order of magnitude larger than ions size. This charge interaction allows nanofiltration to separate ions with different valences.

Due to its separation ability, nanofiltration has become an important process for various applications, including pulp processing [1], water purification [4], demineralization of whey in the dairy industry [5], organics concentration [6], and water softening [7] Table 1 was summarized the most common applications of nanofiltration in the industry.

As can be seen in Fig. 1, in the last two decades, there was increasing published research related to nanofiltration for both modeling and simulation subject.

Nanofiltration membranes can be produced in various configurations such as a spiral wound, plate, and frame, hollow fiber, capillary and tubular with a wide range of materials, including cellulose derivatives, synthetic polymers, inorganic materials and a hybrid of organic and inorganic. The spiral wound module (SWM) design was originally made exclusively for water desalination, but due to its compact design (high packing density), adequate fouling resistance and low price, it became attractive for other industries such as dairy industry and pulp and paper industry [51]. In SWMs, the feed flows through a narrow channel between two membrane sheets in the axial direction. The membranes are glued along three sides to form leaves and are wound around a permeate collecting tube to which the fourth side, the unsealed edge of the leaf, is attached. Inside leaves permeate spacer is located to support the membrane and to direct the permeate stream spirally to the permeate collecting tube. The configuration is shown in Fig. 2.

Many researchers have developed mathematical models to properly design and predict the performance of nanofiltration on the salt separation process. Several models are available in open literature; models most commonly used to describe nanofiltration processes are [53]:

- Solution–diffusion model (SDM) [55]
- Irreversible thermodynamic equations of Kedem and Katchalsky [63]
- Spiegler–Kedem model [66]
- Extended Nernst–Planck model [77]
- Maxwell–Stefan model [101]

Numerous reviews related to the nanofiltration process can be found in the literature. However, a specific review on the comparison of mathematical models for transfer via nanofiltration membranes can hardly be found. This paper has reviewed 24 mathematical models for transport in the nanofiltration process, such as solution–diffusion models, irreversible thermodynamics (IT) models, extended Nernst–Planck equation, and the Maxwell–Stefan model. Fig. 3 schematic the most common models used to describe the transfer phenomena within nanofiltration membranes.

Table 1
Application of nanofiltration in the industry

Industry	Application
Food	Demineralization of whey [5,8,9]
	Demineralization of sugar solutions [10]
	Separation of sunflower oil from solvent [11]
	Recovery of regeneration liquid from decoloring resins in sugar industry [12,13]
Textile, clothing and leather, paper and graphical	Effluent treatment [14]
	Purification of organic acids [15–17]
	Separation of amino acids [18]
	Recovery of water and salts from wastewater [19–21]
	Recovery and reuse of chromium(III) and chromium(II) [22,23]
	Recovery of water from wastewater or wastewater treatment effluent [24–26]
Chemical	Recovery of bleaching solution [27–29]
	Sulfate removal preceding chlorine and NaOH production [30]
	Preparation of bromide [31]
Metal plating and product/ electronic and optical	Recovery of Cu-ions from ore extraction liquids [32]
	Removal of degreasing agents from water [33]
	Removal of precursors of disinfection by-products [34]
Water production	Hardness removal [35,36]
	Removal of natural organic matter (a.o. color) [37–39]
	Removal of pesticides [40]
	Removal of heavy metals (As, Pb), Fe, Cu, Zn and silica [41,42]
	Treatment of brackish water [43]
Landfills, agriculture	Removal of phosphate, sulfate, nitrate and fluoride [44–47]
	Removal of algal toxins [48]
	Purification of landfill leachate [49]
	Removal of selenium from drainage water [50]

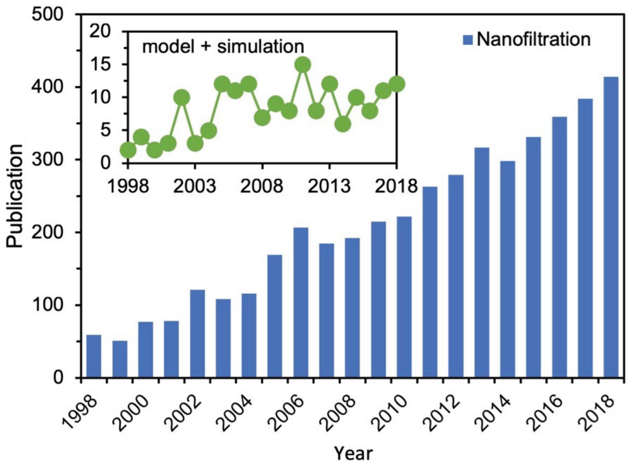

Fig. 1. Publications related to nanofiltration in the last two decades (indexed by Scopus: Nanofiltration Technology; January 26th, 2019).

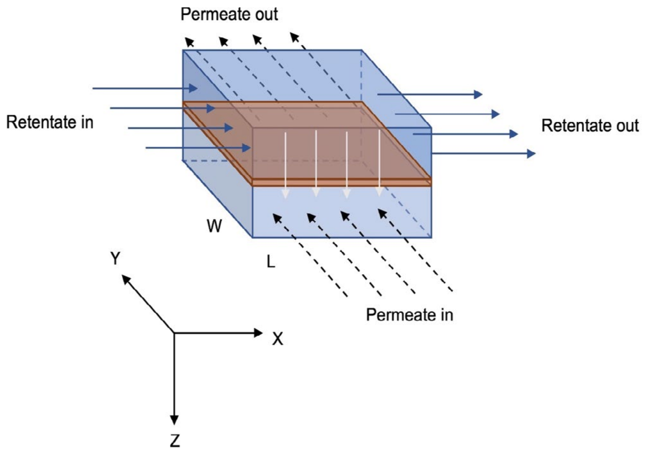

Fig. 2. Representation of an elemental volume of a spiral wound membrane module. (Adapted from Roy et al. [113], Shi et al. [52], and Al-Obaidi and Mujtaba [117]).

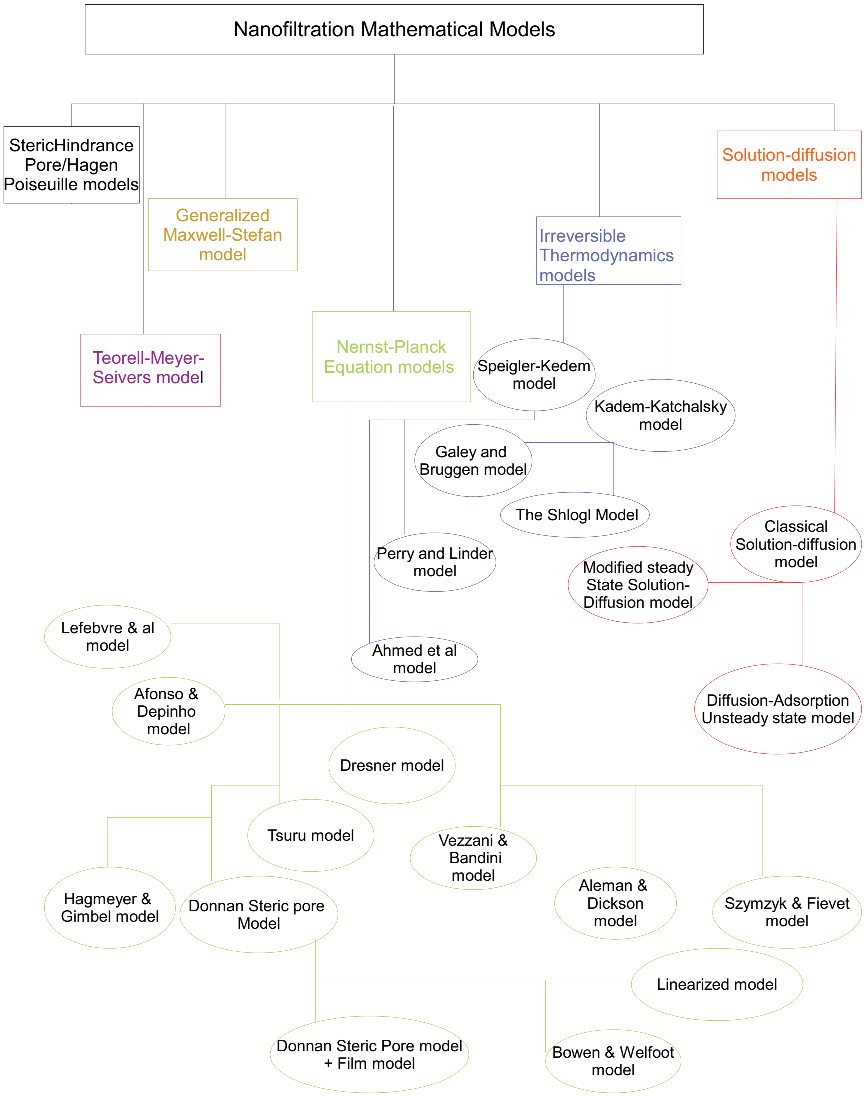

Fig. 3. Nanofiltration mathematical models.

2. Solution–diffusion model

2.1. Classical solution–diffusion model

In solution–diffusion model, each solute dissolves in the membrane at the high-pressure side and diffuses through the membrane in response to the concentration and pressure gradients, without any coupling between the individual fluxes [54,55], the main assumptions characterized this model are:

- Membrane is ideal: nonporous, homogeneous, continuum medium. The solutes dissolve inside the membrane and diffuse through it due to the chemical potential gradient.
- There is chemical equilibrium at phase interfaces.
- The solute and water fluxes are not coupled [56].

The solution–diffusion model supposes that the pressure within a membrane is uniform and that the chemical potential across the membrane is expressed only as gradient of concentration [54,56], Fig. 4 shows the permeation of one solute through the membrane as a solution–diffusion model.

In the review presented by Wijmans and Baker [56] which they detailed the transport within a membrane using the solution–diffusion model, they supposed that the driving forces of pressure, temperature, concentration, and electro-motrice force are interrelated and that the overall driving force producing movement of a permeant is the gradient in its chemical potential.

The flux can be described according to the chemical potential as:

$$J_i = -L_i \frac{d\mu i}{dx} \tag{1}$$

where $d\mu_i/dx$ is the gradient in chemical potential of solute i and L_i is a coefficient of proportionality linking this chemical potential driving force with flux.
where

$$d\mu_i = R_g \cdot T\ln\left(\gamma_i \cdot C_i\right) + V_i dP \tag{2}$$

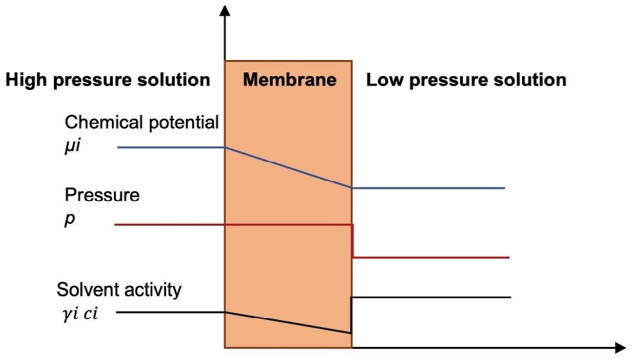

Fig. 4. Pressure-driven permeation of a one-component solution through a membrane according to the solution–diffusion model (Adapted from Wijmans and Baker [56] and Vandezande et al. [119]).

$$\mu_i = \mu_i^0 + R_g \cdot T\ln\left(\gamma_i \cdot C_i\right) + V_i\left(P_i - P_i^0\right) \tag{3}$$

where P_i^0, μ_i^0, γ_i and V_i are the reference pressure, the chemical potential of solute i at a reference pressure, the activity coefficient for the solute i and molar volume of solute i respectively.

The combination of the Eqs. (2) and (1) yields:

$$J_i = -\frac{R_g \cdot T \cdot L_i}{C_i}\frac{dCi}{dx} \tag{4}$$

According to Fick's law where the term ($R_g \cdot T \cdot L_i / C_i$) can be replaced by the diffusion coefficient D_i.

If the membrane compaction is negligible and the solution is diluted, the flux is linearly proportional to the net pressure difference by the proportionality constant, namely pure water permeability A. Membrane constant can be determined from the measurements of pure water flux as a function of transmembrane pressure. The resulting equation is the water flux after many rearrangements to Eq. (4):

$$J_w = A\left(\Delta P - \Delta\pi\right) \tag{5}$$

In the case of the application of Fick's law assumes that the solute flux is not moved by the pressure gradient we obtain the equation of salt flux as:

$$J_s = B\Delta C_s \tag{6}$$

where $A = D_w \cdot C_w \cdot V_w / R_g T \cdot 1/\Delta x$ and $B = (D_s \cdot K_s / \Delta x)$ can be represented respectively as the pure water permeability and solute permeability.

From Eqs. (5) and (6) we noticed that the rejection approaches unity with increasing pressure.

For the very large pressures ($\Delta P \to \infty$) the assumption of $V_s \ll RT\ \Delta(\ln C_s)$ is no longer fulfilled. From Eq. (1) the concentration in the low-pressure side was assumed [55]:

$$C_{\mathrm{sp}} = J_s \cdot \frac{C_w}{J_w} = \frac{\left(D_s \cdot C_{\mathrm{sm}} \cdot V_s \cdot C_{\mathrm{wm}}\right)}{\left(D_w \cdot C_{\mathrm{wm}} \cdot V_w\right)} \tag{7}$$

While the maximum retention can be given as:

$$R = 1 - \left(\frac{C_{\mathrm{sm}}}{C_{\mathrm{sf}}}\right) = 1 - \frac{K_s}{K_w} \cdot D_s \frac{V_s}{D_w} V_w \tag{8}$$

Here K_s and K_w are the distribution coefficients of solute and water, respectively, between the total membrane phases and bulk solution [55].

2.2. Modified steady state solution–diffusion model

The classical form of solution–diffusion model can be written as Eq. (9) [57–59]:

$$J_w = \frac{D_w \cdot C_{\mathrm{wm}} \cdot V_w}{R_g \cdot T \cdot \delta}\left(\Delta P - \Delta\pi\right) = A\left(\Delta P - \Delta\pi\right) \tag{9}$$

The solution–diffusion model, assumes that both solute and water transport across the membrane occurs by diffusion; for organics that can be strongly sorbed in the membrane [57–59] was supposed that the total concentration in the membrane C_{tm} equal to the total concentration of water and solute in the membrane:

$$C_{\text{tm}} = C_{\text{sm}} + C_{\text{wm}} \tag{10}$$

If the above equation is substituted into Eq. (9), we got the following expression:

$$J_w = \left(\frac{C_{\text{tm}} - C_{\text{wm}}}{C_{\text{tm}}}\right) \cdot \frac{C_{\text{tm}} \cdot D_w V_w}{R_g \cdot T \cdot \delta}\left(\Delta P - \Delta\pi\right) = \left(1 - \frac{C_{\text{wm}}}{C_{\text{tm}}}\right) \cdot A^*\left(\Delta P - \Delta\pi\right) \tag{11}$$

where A^* is a new permeability constant and does not depend on the water concentration in the membrane but instead the total concentration in the membrane.

The term of $C_{\text{wm}}/C_{\text{tm}}$ can be defined by the Langmuir type:

$$\frac{C_{\text{wm}}}{C_{\text{tm}}} = \frac{b_0 \cdot C_f}{1 + b_0 \cdot C_f} \tag{12}$$

This upon substitution in Eq. (11), results in:

$$J_w = \left(1 - b_0 \cdot \frac{C_f}{1 + b_0 \cdot C_f}\right) \cdot A^*\left(\Delta P - \Delta\pi\right) = \frac{1}{1 + b_0 \cdot C_f} A^*\left(\Delta P - \Delta\pi\right) \tag{13}$$

The value of A^* was calculated using the distilled water flux of the membrane and Eq. (13):

$$A^* = \frac{J_{w0}}{\Delta P} \tag{14}$$

Eq. (13) indicates that the flux of water through the membrane depends on two parameters, the initial solute concentration as well as the effective pressure driving force. In the presence of the concentration polarization, C_f must be replaced with the wall concentration.

In dilute systems, the solute transport across the membrane can be defined by their diffusion as:

$$J_s = \frac{D_s}{\delta}\left(C_{\text{smf}} - C_{\text{smp}}\right) \tag{15}$$

Langmuir isotherm was used to determine the partition as in the case of water flux equation:

$$C_{\text{smf}} = C_{\text{tm}} \cdot b_0 \cdot \frac{C_f}{1 + b_0 \cdot C_p} \tag{16}$$

$$C_{\text{smp}} = \frac{C_{\text{tm}} \cdot b_0 \cdot C_p}{1 + b_0 \cdot C_p} \tag{17}$$

which when substituted in Eq. (14) results in:

$$J_s = D_s \cdot \frac{C_{\text{tm}}}{\delta}\left(\frac{b_0 \cdot C_f}{1 + b_0 \cdot C_f} - \frac{b_0 \cdot C_f}{1 + b_0 \cdot C_p}\right) = B^*\left(\frac{b_0 \cdot C_f}{1 + b_0 \cdot C_f} - \frac{b_0 \cdot C_p}{1 + b_0 \cdot C_p}\right) \tag{18}$$

where B^* represents a solute permeability constant.

The value of b_0 was determined using the experimental water flux and concentrate concentration using Eq. (13) (with $C_f = C_c$).

Based in the case of the modified solution–diffusion model (MSD), both Eqs. (13) and (18) correspond to the water and solute fluxes across the membrane. Were found the permeate concentration from the substitution of $C_p = J_s/J_w$ and solving the quadratic equation for J_s [60].

2.3. Diffusion–Adsorption unsteady state model

Some solutes can adsorb in the membrane pores as these are transported across the membrane and, as a result, transient behavior is observed in the permeate concentration. A diffusion–adsorption (DA) model has been implemented by Williams et al. [60] to describe this solute transport behavior in which they assumed the water and solute transport occurs by uncoupled diffusion across the membrane.

Fig. 5 shows a cross-section of the RO membrane with solute flux J_s, taking into account Δz as a material balance of the membrane [60].

According to the Fick's law were described J_s, then was obtained as:

$$\frac{\partial C_{\text{sm}}}{\partial t} = D_s \cdot \frac{\partial^2 C_{\text{sm}}}{\partial z^2} - \frac{\partial q_m}{\partial t} \tag{19}$$

Eq. (19) along with an expression for the rate of adsorption (adsorption rate = $\partial q_m/\partial_t$) describes the concentration of solute in the membrane. Before the membrane feed was introduced, there is no solute in the membrane, thus the initial condition can be written as:

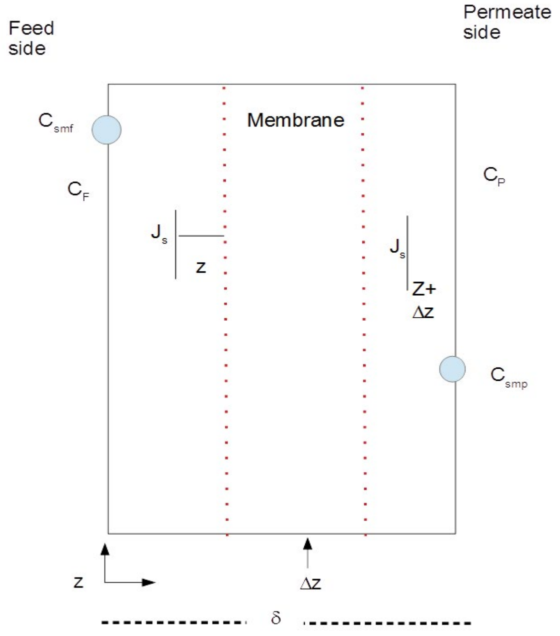

Fig. 5. Schematic illustration of flux and solute partitioning on membrane cross-section (Adapted from Williams et al. [60], Garba et al. [118], and Spiegler and Kedem [66]).

$$C_{\mathrm{sm}(0,z)} = 0 \tag{20}$$

The same boundary conditions were obtained as in the MSD model:

$$C_{\mathrm{smf}} = C_{m(t,0)} = \frac{C_{\mathrm{tm}} \cdot b_0 \cdot C_f}{1 + b_0 \cdot C_f} \tag{21}$$

$$C_{\mathrm{smp}} = C_{m(t,\delta)} = \frac{C_{\mathrm{tm}} \cdot b_0 \cdot C_p}{1 + b_0 \cdot C_p} \tag{22}$$

For the case of the dilute system, the permeate concentration can be removed from Eq. (22) utilizing:

$$C_p = \frac{J_s}{J_w} \tag{23}$$

Along with the evaluation of J_s (using Fick's law) at $Z = \delta$.

Eqs. (19)–(21) and the modified $C_m(t,\delta)$ equation can be rewritten using the transformation ($x = Z/\delta$ and $D_e = D_{\mathrm{sm}}/\delta^2$), these equations then become:

$$\frac{\partial C_{\mathrm{sm}}}{\partial t} = D_e \cdot \frac{\partial^2 C_{\mathrm{sm}}}{\partial x^2} - \frac{\partial q_m}{\partial t} \tag{24}$$

$$C_{\mathrm{sm}(0,x)} = 0 \tag{25}$$

$$C_{\mathrm{sm}(t,0)} = \frac{C_{\mathrm{tm}} \cdot b_0 \cdot C_f}{1 + b_0 \cdot C_f} \tag{26}$$

$$C_{\mathrm{sm}(t,1)} = \frac{-C_{\mathrm{tm}} \cdot b_0 \cdot D_e \cdot \delta \cdot \left.\dfrac{\partial C_{\mathrm{sm}}}{\partial x}\right| x = 1}{J_w - b_0 \cdot D_e \cdot \delta \cdot \left.\dfrac{\partial C_{\mathrm{sm}}}{\partial x}\right| x = 1} \tag{27}$$

The concentration of permeate can be found by reformulating Eq. (17) with the same modification.

If the equilibrium between the adsorbed and non-adsorbed diffusing solute is assumed to exist within the membrane, several adsorption isotherms can be used to describe the solute adsorption in the membrane [60]. If were taken Henry's law in this case, the DA model changed to DA–HA model:

$$q_m = q_0 \cdot C_{\mathrm{sm}} \Rightarrow \frac{\partial q_m}{\partial t} = q_0 \cdot \frac{\partial C_{\mathrm{sm}}}{\partial t} \tag{28}$$

$$\frac{\partial C_{\mathrm{sm}}}{\partial t} = \frac{D_e}{1 + q_0} \frac{\partial^2 C_{\mathrm{sm}}}{\partial x^2} \tag{29}$$

If the Langmuir adsorption isotherm was supposed, we found:

$$q_m = q_1 \cdot b_1 \cdot \frac{C_{\mathrm{sm}}}{1 + b_1 \cdot C_{\mathrm{sm}}} \Rightarrow \frac{\partial q_m}{\partial t} = q_1 \cdot \frac{b_1}{\left(1 + b_1 \cdot C_{\mathrm{sm}}\right)^2} \frac{\partial C_{\mathrm{sm}}}{\partial t} \tag{30}$$

Thus, the DA model can be transformed into the DA–LA model:

$$\left[1 + \left(q_1 \cdot \frac{b_1}{\left(1 + b_1 \cdot C_m\right)^2}\right)\right] \frac{\partial C_m}{\partial t} = D_e \cdot \frac{\partial^2 C_m}{\partial x^2} \tag{31}$$

To determine D_s for DA–HA and DA–LA models, it was supposed that the diffusion of the solute in the membrane takes place through the water dissolved in the membrane polymers. Since the effective diffusivity of organic solutes through the membrane is unknown, the following equation was used to calculate the value D_s:

$$D_s = \frac{D_w}{b} \tag{32}$$

"b" is Ferry–Faxen-type friction parameter; was estimated by Sourirajan and Matsuura [61] as:

$$b = 44.57 - 416.2\lambda + 934.9\lambda^2 + 302.4\lambda^3 \tag{33}$$

where $\lambda = r_s/r_p$ and it's valid for the interval of $0.22 < \lambda < 1$; the diffusivities D_s for the solutes in water were calculated using the Wilke–Chang estimation method and Stoke's radius (r_s) for each solute.

If we work with a batch membrane system, it should include the evolution of both volume and concentration changes against time so solute material balance results in:

$$dC_c \cdot \frac{V_c}{dt} = 0 - S \cdot J_w \cdot C_p - \frac{dq_m}{dt} \tag{34}$$

where q_{tm} defined as the membrane total solute adsorption and Eq. (34) can be expanded to:

$$V_c \cdot \frac{dC_c}{dt} + C_c \cdot \frac{dV_c}{dt} = -S \cdot J_w \cdot C_p - \frac{dq_m}{dt} \tag{35}$$

In which the water material balance is given, as:

$$Y_p = \frac{V_p}{V_f} \tag{36}$$

Then

$$V_c = V_f \cdot \left(1 - Y_p\right) \Rightarrow \frac{dV_c}{dt} = -V_f \frac{dY_p}{dt} \tag{37}$$

and

$$\frac{dY_p}{dt} = S \cdot \frac{J_w}{V_f} \tag{38}$$

Combining Eqs. (37) and (38):

$$\frac{dV_c}{dt} = -S \cdot J_w \tag{39}$$

Substituting Eqs. (39) and (36) into Eq. (35) and rearranging results in:

$$\frac{dC_c}{dt} = \frac{S \cdot J_w \cdot C_c - S \cdot J_w \cdot C_p - \frac{dq_m}{dt}}{V_f\left(1 - Y_p\right)} \tag{40}$$

The system of Eqs. (38) and (40) along with an expression for the adsorption in the membrane, the water flux, solute flux (J_w, J_s) and concentration of permeate (C_p) describe the batch membrane system taking into account the conditions of the initial state.

The permeate concentration C_p value obtained from RO transport models is instantaneous permeate concentration with time *t*. The cumulative permeate concentration for a batch process is represented as the concentration of the total collection of permeate volume, according to a specific time or at a specific water recovery [60] it is calculated as:

$$C_{\text{pc}} = \frac{\int_0^{V_p} C_p \cdot dV_p}{\int_0^{V_p} dV_p} \approx \frac{\sum_{i=1}^{N} C_p \cdot \Delta V_p}{\sum_{i=1}^{N} \Delta V_p} \tag{41}$$

3. Irreversible thermodynamics models

Irreversible thermodynamic models are used to describe transport on the membrane as an irreversible process that continuously produces entropy and dissipates free energy. This class of models is useful, especially when the membrane structure is not known and the mechanism of transport within the membrane is not fully understood. Although less information is required to set-up the models [62].

3.1. Kedem–Katchalsky model

Based on dilute solution of two non-electrolyte solutes Kedem and Katchalsky [63] were developed, new formalism to handle the case where water and solute transport across the membrane is physically coupled, typically by co-transport through a single species of pores.

In this case, the water flux physically interacts with solute flux, with the degree of interaction that can be characterized by a reflection coefficient, σ. In which this model based on three parameters, the hydraulic permeability *A*, solute permeability *B*, and reflexion coefficient σ where they are constant and independent of each other to maintain the interactions between solute, water, and the membrane, with linear variation of both pressure and concentration gradients for lower solvent flow rates.

In the Kedem–Katchalsky model, the relation of the volume flux (J_v) and the solute flux (J_s) through a membrane is defined as:

$$J_v = A \cdot \left(\Delta P - \Delta\pi\right) \tag{42}$$

where

$$\Delta\pi = R \cdot T \cdot \Delta C = R \cdot T \cdot \left(C_{\text{ms}} - C_{\text{ps}}\right) \tag{43}$$

$\Delta\pi$ is the osmotic pressure difference, R_g is the constant of ideal gazes, T is the temperature and ΔC is the solute concentration difference, while C_{sm} and C_{sp} are corresponded to the concentration of solute at the membrane and permeate phases, respectively.

where the solute flux J_s is defined by:

$$J_s = B \cdot \Delta\pi_s + C_s^{\text{ave}} \cdot (1 - \sigma) \cdot J_w \tag{44}$$

where C_s^{ave} represents an average concentration of solute that can be written as:

$$C_s^{\text{ave}} \approx \frac{C_{\text{fs}} + C_{\text{smf}}}{2} \tag{45}$$

Case of dilute solution

So the solute flux can be given in the way as:

$$J_s = \underbrace{B \cdot R_g \cdot T \cdot \left(C_{\text{sm}} - C_{\text{sp}}\right)}_{\substack{\uparrow \\ \text{Diffusive solute flux}}} + \underbrace{C_s^{\text{ave}} \cdot (1 - \sigma) \cdot J_w}_{\substack{\uparrow \\ \text{Solute transport by convection}}} \tag{46}$$

Diffusive solute flux Solute transport by convection

The solute rejection *R* can be written as:

$$R = 1 - \frac{C_{\text{sp}}}{C_{\text{smf}}} = 1 - \frac{J_s}{J_w \cdot C_{\text{smf}}} \tag{47}$$

3.2. Schlögl model

Schlögl [64] developed a model in which he derived an integral formula for particle fluxes, starting from the very general equation based on the Kedem–Katchalsky model and integrating them across the membrane. In which he discussed only the isothermal system for stationary case in his work, taking into account the case of dilute solutions.

Both fluxes of (solute and water) for a dilute mixture solutions is given as:

$$J_{\text{si}} = C_i'(1 - \sigma)J_w + \sum_{j=1}^{n} A_{ij}\Delta C_j \left(j = 1\ldots\ldots..n\right) \tag{48}$$

where A_{ij} is solute–solute interaction and refers to the concentration difference of other solutes in the system, while the water flux can be illustrated by:

$$J_w = A\left(\Delta P - \sum_j \sigma_j C_j X_j^+\right) \tag{49}$$

$$X_j^+ = \left(X_j - \frac{V_j}{V_w} X_w\right) \tag{50}$$

X_j, V_j, X_w, and V_w are respectively the molar fraction and the mean molar volume of solute *j* and water.

Then Eq. (50) describes the expression of the ion flux of solute at the point (*x*) of the membrane surface, as:

$$J_{\text{si}} = C_i'(1 - \sigma)J_w - \sum_{j=1}^{n} D_w K_j \frac{dC_j(x)}{dx} j = 1\ldots n \tag{51}$$

where D_w represents the membrane diffusion coefficient that writing as $D_w = A_{ij} \cdot l / K_j$, K_j represents partition coefficient of j and A_{ij} is the permeability coefficient between two solutes (i–j), l is the membrane length.

The integration of the above equation across the membrane thickness yields to:

$$J_{\mathrm{si}} = C_i'\left(1-\sigma\right)J_w + A_i z_i \frac{C_i' F}{R_g T}\Delta\vartheta + A_i \frac{V_i}{\sinh V_i}\left(C_{\mathrm{smf}} - C_{\mathrm{smp}}\right) \tag{52}$$

where $C_i' = (C_{\mathrm{smf}} + C_{\mathrm{smp}})/2$, $C_{\mathrm{smf}} = C_i' + 0.5\Delta C_i$.
F, z_i and $\Delta\vartheta$ are respectively the Faraday's constant, the charge of valence of solute i and the electrical potential difference.

$$J_w = A\left(\Delta P - \Delta\pi\right) - A R_g T \sum_i \sigma \frac{V_i}{\sinh V_i}\left(C_{\mathrm{smf}} - C_{\mathrm{smp}}\right) \tag{53}$$

These equations are more accurate expressions than alluded to before by containing a new term $V_i/\sinh V_i$ which describes the non-linearity between the fluxes of solutes and the driving forces.

3.3. Galey and Van Bruggen model

Galey and Van Bruggen [65] extended the Kedem–Katchalsky model for multi organic solutes in dilute solution by using three different membranes, in their work Galey and Van Bruggen [65] showed that an existing interaction caused by the solute flux in which this interaction is related to three parameters (solute permeability, concentration, and molecular size).

The expression of flux for solutes i and j in a dilute solution of multi-solutes can be given:

$$J_{\mathrm{si}} = C_i'\left(1-\sigma\right)J_w + A_{ii}\Delta C_i + A_{ij}\Delta C_{ji\sim j} \tag{54}$$

where J_{si} can be obtained by rotating the i to j; ω_{ij} represents the solute-solute interaction given by the coefficient of cross-permeability between solutes, while A_{ii} is the self-permeability coefficient of solute i. Also, ΔC_i and ΔC_j are the concentration differences of solutes i, j across the membrane.

Eq. (54) can be modified to indicate the solute flux in the multi-component mixture as:

$$J_{\mathrm{si}} = C_i'\left(1-\sigma\right)J_w + A_{ii}\Delta C_i + \sum\nolimits_{j=0, j\neq 1}^{n} A_{ij}\Delta C_j \tag{55}$$

$$\left(J_{\mathrm{si}} = \frac{A_{ij}}{A_{jj}} J_{\mathrm{sj}}\right) \tag{56}$$

where the reflection coefficient σ can be defined as:

$$\sigma = \frac{\pi}{\Delta \mathrm{CRT}} \tag{57}$$

where π is the observed osmotic pressure, and ΔCRT represents the Van't Hoff osmotic pressure given as in Eq. (43).

Eq. (56) describes the impact of the solute flux of j on the flux of solute i in term of concentration difference, the new term of self and cross permeability coefficients. In which Galey and Van Bruggen [65] stated that this new term named effective permeability coefficient A_{ij}/A_{jj} increase with decrease of pore size.

3.4. Spiegler–Kedem model

The classical Spiegler–Kedem model [66] was developed based on IT. It provides a simple framework to describe solute transport in both RO and nanofiltration processes. In the Spiegler–Kedem model, the membrane is regarded as a "black-box" that can be characterized in terms of two coefficients: the solute permeability (B) and the reflection coefficient (σ). Spiegler–Kedem model [66] is different from the traditional solution–diffusion model. The traditional solution–diffusion model is based on the primary assumption that the solute and water flux are independent of each other, while the Spiegler–Kedem model considers convective coupling of solute and water species. Solute transport occurs predominantly via diffusion in the RO membrane, while for "looser" membranes such as nanofiltration, both the convective and diffusive contributions to the solute flux are important and cannot be ignored.

In which the water and the solute fluxes must take into account the difference concentrations profile at different flow rates, in this context Eqs. (42) and (46) can be transformed into [66]:

$$J_v = -A^*\left(\frac{dP}{dx} - \sigma\frac{d\pi}{dx}\right) \tag{58}$$

$$J_s = -B^*\frac{dC_s}{dx} + \left(1-\sigma\right)C_s \cdot J_v \tag{59}$$

where

$$A = \frac{A^*}{\Delta x} \tag{60}$$

and

$$B = \frac{B^*}{R_g \cdot T \cdot \Delta X} \tag{61}$$

A^*, B^* are respectively the local water permeability and the local solute permeability coefficients.

Reflection coefficient σ, which represents the selectivity of a membrane for the solute it can be determined when the osmotic pressure difference is compensated by the hydraulic pressure difference where no permeate flux is observed:

$$\sigma = \frac{\Delta P}{\Delta\pi}\bigg| J_p = 0 \tag{62}$$

For an unselective membrane (σ = 0) osmotic pressure effect in Eq. (58) disappears and solute convective transport is predominant. Whereas, for an ideal semi-permeable membrane (σ = 1), water flux definition turn to the one in SDM and convective salt transport vanishes.

By integrating Eqs. (58) and (59) over the membrane thickness Δx and implementing in the rejection equation gives:

$$R = \frac{\left(1-m\right)\cdot\sigma}{1-\sigma\cdot m} \tag{63}$$

where m is:

$$m = \exp\left(\left(\sigma-1\right)\cdot J_w\cdot\frac{\Delta x}{B^*}\right) \tag{64}$$

B^* and σ can be determined by measuring the solute rejection as a function of water flux. Eq. (64) is a difference in comparison to the SDM since with an increase in water flux the rejection approaches to the reflection coefficient σ. We noticed that the concentration dependence on rejection was considered in the model developed by Schirg and Widmer [67].

3.5. Perry and Linder model

Perry and Linder [68] used a modified thin-film composite membrane endowed with high rejection to low molecular weight organic and high salt passage to describe the interaction between the mixture of salts and organic ion on the membrane performance, in which they extended Spiegler–Kedem model for the effluent solution of (mixture of salt and organic solutes), in their study Perry and Linder [68] observed high negative salt rejection value when charged organic solutes are concentrated or purified under this membrane.

In their study, it was assumed that a constant value of both permeability and reflection coefficient with no concentration polarization effect, as shown by the following equations of rejection rate:

$$R = \frac{\left(1-\sigma\cdot m\right)-\left(1-\sigma\right)\left[\dfrac{1+\gamma C_X^-}{C_s'}\right]^{0.5}}{1-\sigma\cdot m} \tag{65}$$

where C_X^- and C_s', γ are respectively organic solute concentration in the solution, the salt concentration in the feed and the number of charge groups from the organic ion. This equation can express the impact of organic ion concentration C_X^- and the flow parameter m as shown in Eq. (64) with, $(1 + \gamma C_X^-/C_s')^{0.5} = \alpha$.

Eq. (65) can be rewritten as:

$$R = 1-\frac{\left(1-\sigma\right)\cdot\alpha}{1-\sigma\cdot m} \tag{66}$$

The above transforms to Eq. (64) for pure salt, where C_X^- = zero and α = one.

The observation of Perry and Linder [68] study showed that the presence of organic ions in saline electrolyte solution could sustain an impact on promoting by the organic ion rejection in spite of negative salt rejection.

3.6. Ahmad et al. [69] model

According to Spiegler–Kedem model, Ahmad et al. [69] developed a new form of a one-dimensional model for mixture system filtration in which Ahmad et al. [69] extended the Spiegler–Kedem model with incorporation of the solute-solute interaction.

In addition, were proposed a new equation to calculate the water and solute fluxes for a multi-ions system. They did this by integrating their model over the membrane thickness and considered the effects of concentration polarization in their model.

To valid it this model they took six assumptions by consideration:

- Each solute exist in the system are semi-permeable to the membrane.
- Each solute exist in the system can be either the neutral ions or salts ions. The extended Spiegler–Kedem model was assumed to adequately predict both transports of solutes and water regardless, the type of solvent, membrane or solutes and its charges.
- Each solute will have its independent value of the diffusion and mass transfer coefficients in the concentration polarization layer thickness.
- The pressure and concentration gradients are driving forces.
- The water transport was related to the interaction solute–water, solutes concentration, and membrane properties.
- The solute transport was related to the interaction solute–water, solute concentration, membrane properties, and solute–solute interactions.

The expressions of water and solute fluxes, which are controlled by the water and solute forces for a multi-ions system, are represented as shown below:

$$J_w = A_{\text{ww}}\cdot F_w\cdot\sum\nolimits_{s=1}^{n} A_{\text{ws}}\cdot F_s \tag{67}$$

$$J_s = B_{\text{sw}}\cdot F_w + \sum\nolimits_{i=1}^{n} B_{\text{si}}\cdot F_i,\quad i = 1,2,3,\ldots,n \tag{68}$$

where F_s, F_i and F_w are the exerted driving forces of solutes s and solute i and water respectively.

The total flux of the volume was written as:

$$J_w = -A_{\text{ww}}\cdot V_w^2\left[\frac{dp}{dx}-\sum\nolimits_{s=1}^{n}\left(1-\left(\frac{A_{\text{ws}}\cdot C_w}{A_{\text{ww}}\cdot C_i}\right)\right)\frac{d\pi s}{dx}\right] \tag{69}$$

where C_w is the molar concentration of water:

Eq. (69) can be simplified as:

$$J_w = A^*\left[\frac{dp}{dx}-\sum\nolimits_{s=1}^{n}\sigma\cdot\frac{d\pi s}{dx}\right] \tag{70}$$

where $A^* = -A_{\text{ww}}\cdot V_w^2$,

$$\sigma = \left(1-\frac{A_{\text{ws}}\cdot C_w}{A_{\text{ww}}\cdot C_i}\right) \tag{71}$$

In addition, the total osmotic pressure gradient $d\pi$ for the mixture can be calculated from the summation of the osmotic pressure gradient caused by each solute, $d\pi s$:

$$\frac{d\pi s}{dx} = \sum\nolimits_{s=1}^{n} \frac{d\pi s}{dx} \tag{72}$$

$$d\pi = \sum\nolimits_{s=1}^{n} R_g T (C_i - C_{\mathrm{tm}}) \tag{73}$$

where C_x is solute concentration, C_{tm} is water concentration in the bulk and the permeate sides of the membrane. Van't Hoff's equation [70] was used for the calculation of the osmotic pressure, in the case of a dilute aqueous solution was given as Eq. (43), while the solute flux for each component is written as:

$$J_s = \sum\nolimits_{i=1}^{n} B^*_{\mathrm{si}} \frac{d\pi i}{dx} + (1-\sigma) C_s J_w \left(i = 1,2,3,\ldots,n\right) \tag{74}$$

where ω^-_{s-i} is the local solutes permeability constant of solute s with the consideration of the interaction of the solute i have given as:

$$B^*_{\mathrm{si}} = A_{\mathrm{ws}} \cdot \frac{A_{\mathrm{wi}}}{A_{\mathrm{ww}} \cdot C_i} - \frac{B_{\mathrm{si}}}{C_i} \tag{75}$$

The integration of Eqs. (67) and (43) gives:

$$J_w = A\left[\Delta p + \sum\nolimits_{s=1}^{n} \sigma R_g T R_j C_{s''}\right] \tag{76}$$

$$F_s = C_{\mathrm{smf}} - \frac{C_{\mathrm{sm}}(1-\sigma)}{C_{\mathrm{smf}}\sigma} \tag{77}$$

where C_{sm}, R is the interfacial solute concentration in the membrane and actual rejection of solute, $R = -C_{\mathrm{smp}}/C_{\mathrm{smf}}$, respectively:
where F_s can be written as:

$$F_s = \exp\left[\frac{-J_w(1-\sigma)}{B_{\mathrm{ss}}\left(1 + \sum\nolimits_{i=1}^{n} O_i\right)}\right] \tag{78}$$

where

$$O_i = \frac{B_{\mathrm{si}}\left(C_{\mathrm{smf}} - C_{\mathrm{smp}}\right)\exp\left(\frac{J_w}{k}\right)}{J_w\left[C_{\mathrm{smf}} - (1-\sigma)C_s^{(\mathrm{av})}\right]} \tag{79}$$

$$B_{\mathrm{ss}} = \left(\frac{A^2_{\mathrm{WS}}}{A_{\mathrm{ww}} C_s^{(\mathrm{av})}} - \frac{B_{\mathrm{ss}}}{C_s^{(\mathrm{av})}}\right)\frac{R_g T}{\delta} \tag{80}$$

where B_{ss} is defined as the solute permeability coefficient with itself interaction, B_{si} is defined as the solute permeability coefficient with solute (i) interaction and δ the membrane thickness. $C_s^{(\mathrm{av})}$ is the average concentration of solute. The rearrangement of Eq. (77) gives the expression of (actual rejection) as:

$$R = \frac{\sigma(1-F_s)}{1-\sigma F_s} \tag{81}$$

In the later work of Ahmad et al. [71] were demonstrated the efficiency of this model in the case of multi solute incorporate with a complex organic solution with the determination of each solute concentration.

In the same context, we distinguish several models developed based on the Spiegler–Kedem model in which they incorporate the film theory equation, we could cite briefly:

The Schirg and Widmer model [67] were combined the film theory in the Spiegler–Kedem model taking into account the effect of concentration polarization on both concentrations of permeate and bulk solute, based on this model Wadley et al. [72] developed a new approach for the case of mixture separation of (NaCl + organic ion).

According to the same context, Gupta et al. [73] developed a model for electrolyte dilute binary solution, in which they supposed that the boundary layer thickness over the membrane is constant.

4. Nernst–Planck equation

Nernst–Planck equation is a fundamental equation for ion flux that was introduced by Nernst [74] and perpetuated by Planck [75]. This equation takes into account the electrochemical potential gradient as driving force for electrolyte solutions. It is expressed in the Teorell equation as flux = concentration·mobility·driving force.

Accordingly:

$$J_i = -c_i \cdot \frac{D_i}{R_g T} \cdot \frac{d\mu_i}{dx} \tag{82}$$

After substituting Eqs. (2) and (3) in Eq. (82) we find:

$$J_i = -c_i \cdot \frac{D_i}{R_g T} \cdot \left(R_g T \cdot \frac{d\ln a_i}{dx} + V_i \cdot \frac{dP}{dx} + z_i \cdot F \cdot \frac{d\varphi}{dx}\right) \tag{83}$$

$$J_i = -c_i \cdot \frac{D_i}{R_g T} \cdot \left(R_g T \cdot \frac{1}{c_i} \cdot \frac{dc_i}{dx} + R_g T \cdot d\ln\frac{\gamma_i}{dx} + \bar{V}_i \cdot \frac{dP}{dx} + z_i \cdot F \cdot \frac{d\varphi}{dx}\right) \tag{84}$$

Assuming constant activity coefficient and neglecting pressure terms, Nernst–Planck equation was obtained as follows:

$$J_i = -D_i \frac{dc_i}{dx} - z_i \cdot F \cdot c_i \cdot \frac{D_i}{R_g T} \cdot \frac{d\varphi}{dx} \tag{85}$$

In the difference to the solution–diffusion membranes, a convective solute transport occurs in nanofiltration membranes. Schlögl [76] introduced the convective salt transport along with permeating water in Nernst–Planck equation in 1964.

Nernst–Planck equation models equation accounts for the transport of ions across the membrane by diffusion due to the gradient of concentration, electro-migration caused by a gradient of electrical potential, and convection by the pressure difference as Eq. (86) indicated:

$$J_i = \underbrace{-D_i \frac{dc_i}{dx}}_{\text{Diffusion}} \underbrace{- z_i \cdot F \cdot c_i \cdot \frac{D_i}{R_g T} \cdot \frac{d\varphi}{dx}}_{\text{Electro-migration}} + \underbrace{c_i \cdot v}_{\text{Convection}} \tag{86}$$

Diffusion electro-migration convection.

4.1. Dresner model [77]

Dresner [77] suggested a new method for the integration of the extended Nernst–Planck equation in the hyperfiltration of a multi-ion solution through the ion exchange membrane. This method is based on the assumption of co-ion exclusion, in which Dresner [77] introduced a coupling coefficient β_i in the equation proposed by Schlögl Eq. (87):

$$J_i = J_w \cdot c_i - D_i \cdot \frac{dc_i}{dx} + z_i \cdot c_i \cdot D_i \cdot F \cdot \frac{E}{RT} - c_i \cdot D_i \cdot \frac{d\ln\gamma_i}{dx} \tag{87}$$

To realize the membrane as an active component in mass transport. Accordingly, the interactions between permeating solutes and the membrane are expressed in the convective term. Herewith, velocities of solutes through the membrane were prevented to be the same as the water velocity.

$$J_i = \beta_i \cdot J_w \cdot c_i - D_i \cdot \frac{dc_i}{dx} + z_i \cdot c_i \cdot D_i \cdot F \cdot \frac{E}{R_g T} - c_i \cdot D_i \cdot \frac{d\ln\gamma_i}{dx} \tag{88}$$

Accordingly, when counter-ions are adjacent to the pore surface due to electrostatic attraction, only a fraction of overall concentration can be transported convective. In this case, $\beta_i < 1$ and even can be more decreased in the case that counter-ions are attached to the pore surface.

In addition, co-ions may accumulate in the middle of the pore due to the pore charge exclusion and transported convective with a higher velocity than at pore walls so that $\beta_i > 1$.

In addition to Eq. (88), Dresner [77] introduces the electro-neutrality equations in the membrane:

$$\sum_i z_i \cdot c_i + X_M = 0 \tag{89}$$

And in the external solution:

$$\sum_i z_i \cdot c_i = 0 \tag{90}$$

Since no electric current flow in hyper-filtration:

$$\sum_i z_i \cdot J_i = 0 \tag{91}$$

The condition of thermodynamic equilibrium at each interface membrane/solution occurs the form of:

$$c_i \cdot \frac{\gamma_i}{C_i \cdot \gamma_i} = \exp\left(-z_i \cdot F \cdot \frac{\Delta\varphi}{R_g T}\right) \tag{92}$$

where $\Delta\varphi$ is the potential difference between a point just inside the membrane and the contacting solution (Donnan potential); and about the composition of the filtrate is found it using the fluxes J_i and J:

$$c_p = \frac{J_i}{J_w} \tag{93}$$

If co-ions were eliminated from the membrane, no current for any counter-ion could flow in the steady-state, for then a steady separation of charge would occur in this case J_i, would vanish for each counter-ion, and Eq. (88) could be solved as:

$$\frac{1}{c_i} \cdot \frac{dc_i}{dx} = \beta_i \cdot \frac{J_w}{D_i} + z_i \cdot F \cdot \frac{E}{R_g T} \tag{94) (counter-ion only}$$

$$\ln c_i = \beta_i \cdot \frac{J_w x}{D_i} - z_i \cdot \frac{F\varphi}{R_g T} + \text{cst} \tag{95) (counter-ion only}$$

where $E \equiv -d\varphi/dx$ represents as electrical potential in the feed/membrane interface, so Eq. (95) can written as:

$$c_i = C_{\text{smf}} \exp\left(\beta_i \cdot \frac{J_x}{D_i} - z_i \cdot \frac{F\left[\varphi_b - \varphi_m\right]}{R_g T}\right) \tag{96}$$

The electrical potential φ is given as constant; therefore, in the feed solution, we took $\varphi = 0$ according to Eq. (92):

$$C_{\text{smf}} \cdot \gamma_i = c_{i(x)} \cdot \gamma_{i(x)} \exp\left(-zi \cdot F \cdot \frac{\varphi_b}{R_g T}\right) \tag{97}$$

Then Eq. (96) was written as:

$$c_i \cdot \gamma_{i(r)} = c_{i(x)} \cdot \gamma_{i(x)} \exp\left(\beta_i \cdot \frac{J_x}{D_i} - z_i \cdot F \cdot \frac{\varphi_m}{R_g T}\right) \tag{98}$$

Those equations were used only in the case of counter-ion only.

If we took constants value of activity coefficients γ_i in the membrane, we can find ($\varphi_{(x)}$) using electro neutrality Eq. (89) to Eq. (98):

$$\sum_i{}' z_i \cdot c_i \cdot \frac{\gamma_{i(x)}}{\gamma_i} \exp\left(\beta_i \cdot \frac{J_w x}{D_i} - z_i \cdot F \cdot \frac{\varphi_m}{R_g T}\right) = \sum_i{}' z_i \cdot c_i = -X_M \tag{99}$$

For the case of co-ion currents, in this case, was assumed that the calculation using the electric potential for currents co-ion, the solution of Eq. (88) can be written as:

$$\begin{aligned} &c_i \cdot \gamma_i \exp\left(-\beta_i \cdot \frac{J_w x}{D_i} + z_i \cdot F \cdot \frac{\varphi_m}{R_g T}\right) \\ &= c_i \gamma_{i(x)} - \frac{J_i}{D_i} \gamma_i \int_{0+}^{x} \exp\left(-\beta_i \cdot \frac{J_x}{D_i} + z_i \cdot F \cdot \frac{\varphi_m}{R_g T}\right) dx \end{aligned} \tag{100) Co-ion only}$$

We verified the solution of Eq. (100) by substitution into Eq. (88) or by setting $x = 0+$ which satisfies the boundary conditions at the feed/membrane interface.

The conditions where we have a satisfactory state of affairs for this equation is that the term of $F\cdot\varphi(x)/R_gT$ had the sign of $-q$ and were to increase exactly as rapidly as $\left|\frac{\beta_j}{z_j \cdot D_j}\right| J_w x$, the term on the left-hand side of Eq. (99) for which $i = q$ in which have turned $J_w\, x$ from a finite limit as $J_w\, x$ become infinite, whereas the other terms $i \neq j$ would vanish.

4.2. Tsuru et al. [78] model

Tsuru et al. [78] used Donnan equilibrium at the phase interfaces (Eq. (101)) to account for ion distribution.

$$\left(\gamma_{\text{im}} \cdot \frac{c_i}{\gamma_{\text{ib}} \cdot C_{\text{smf}}}\right) = \exp\left(-z_i \cdot \frac{F}{R_g T} \Delta\varphi_D\right) \quad (101)$$

In nanofiltration membranes, the Donnan effect stems from membrane charge. Expressed simply, the repulsion of co-ions from the charged nanofiltration membrane surface is described by Donnan exclusion; because of electro-neutrality, counter-ions are also rejected and salt retention occurs. Rejections of more permeable monovalent salts are mainly determined by the concentration ratio of the permeable monovalent salt and the retained multivalent salt [79,80]. The difference in concentration of solute between two phases (bulk solution and membrane surface) originated from charge effects between membrane charge and charged ions in the solution, leads to an osmotic pressure difference between the membrane and the solution. A potential difference at the interface compensates this osmotic pressure difference due to the thermodynamic equilibrium The effect of Donnan potential is to repel the co-ion from the membrane was given as follows [79]:

$$\Delta\varphi_D = \varphi_M - \varphi_B = \frac{R_g \cdot T}{z \cdot F} \ln \frac{C_{\text{smf}}}{c_i} \quad (102)$$

where φ_M the potential in the membrane, φ_B is the potential in the bulk, C_i and c_i defined as the concentration of solute i in the bulk and the membrane.

Referring to the Nernst–Planck equation models (ENP) equation by Dresner [77], the effect of the interactions between the cation and the negative membrane charge on the coupling coefficient was interpreted similarly in Tsuru et al. [78] model. However, the anion mobility inside the pore is concluded to be the same as in the bulk solution based on the measurements performed by Kobatake and Kamo [81]. Consequently, a coupling coefficient above 1 is not the case for the anion transport inside the pore. In this model, the mobility in the pore is considered to be the same as in the bulk. Additionally, measurements by Kobatake and Kamo [81] also showed that the activity coefficients relation in the membrane to the bulk is similar to that of the mobility. Therefore, Tsuru et al. [82] considered the same activity coefficients in the membrane and the bulk, $\gamma_{\text{im}}/\gamma_{\text{ib}} = 1$, where the activity coefficients in the bulk are set to 1 [82].

The electro-neutrality conditions in the membrane and the bulk are the same as Eqs. (89) and (90).

The model uses two fitting parameters: the effective membrane charge density (X_M) and the surface porosity to the membrane thickness ratio (ε/δ). The former parameter changes as a function of salt concentration and salt type. In this model, both parameters are calculated by fitting the experimental single salt rejection data to the model. Effective membrane charge density for salt mixtures is described as an additive value of the ones obtained through single salt measurements:

$$X_M = \sum_i \left(X_M\right) i \cdot x_i \quad (103)$$

From the continuity equation in the membrane and the permeate, salt flux is correlated to the permeate concentration and the velocity inside the membrane:

$$J_i = C_p \cdot v \quad (104)$$

Substituting Eq. (104) in Eq. (86) and applying the electro-neutrality conditions, two first-order differential equations (ODE) for the concentration and the potential gradients are obtained. These equations are solved numerically, by the Runge–Kutta method.

4.3. Donnan steric pore model

Several models used to describe the separation within nanofiltration membranes, among those models the use of extended Nernst–Planck equation is best known for predicting ion transport [77]. This equation describes the ions transport across the membrane by taking into account three main mechanisms: diffusion, electro-migration and convection this due to concentration, electric potential gradient and the pressure difference across the membrane respectively. Donnan steric pore model (DSPM) was introduced by Bowen and Mukhtar [83]. The model considers the membrane as having the cylindrical pores and necessitates three parameters of the membrane; the effective radius of membrane pore (r_p), the ration of effective membrane thickness to the porosity (δ/ε) and the effective membrane charge density (X_M). A prior membrane characterization is essential to determine the structural parameters. The effective pore radius can be determined through an approach based on the continuum hydrodynamic models proposed by Ferry [84] by using the uncharged solute rejection data where the charge effects can be ignored. The distributions of the ions at the membrane interfaces are expressed through both the Donnan and the steric effects (Donnan-steric partitioning):

$$\frac{c_i}{C_{\text{smf}}} = \theta_i \cdot \exp\left(-z_i \cdot \frac{F}{R_g T} \cdot \Delta\varphi_D\right) \quad (105)$$

where θ is the steric hindrance factor defined as:

$$\theta_i = \left(1 - \lambda_i\right)^2 = \left(1 - \frac{r_s}{r_p}\right)^2 \quad (106)$$

The ion transport can be described by the ENP equation, which is modified to include the hindered transport inside pores due to the pore geometry:

$$J_i = -D_{\text{ip}} \cdot \frac{dc_i}{dx} - z_i \cdot F \cdot c_i \cdot \frac{D_{\text{ip}}}{R_g T} \frac{d\varphi}{dx} + K_{\text{ic}} \cdot c_i \cdot v \tag{107}$$

K_{ic} is the hindrance factor for convection.

$$K_{\text{ic}} = \left(2 - \theta_i\right) \cdot \left(1 + 0.054\lambda_i - 0.988\lambda_i^{\,2} + 0.441\lambda_i^{\,3}\right) \tag{108}$$

Pore diffusivity is defined as:

$$D_{\text{ip}} = K_{\text{id}} \cdot D_{\text{ib}} \tag{109}$$

where K_{id} is the hindrance factor for diffusion.

$$K_{\text{id}} = 1 - 2.3\lambda_i + 1.154\lambda_i^{\,2} + 0.224\lambda_i^{\,3} \tag{110}$$

The concentration gradient of solute i in a solution can be derived from Eq. (107) by applying Eq. (104) as:

$$\frac{dc_i}{dx} = \frac{v}{D_{\text{ip}}} \cdot \left(K_{i,c} \cdot c_i - C_{\text{smp}}\right) - z_i \cdot F \cdot \frac{c_i}{R_g T} \cdot \frac{d\varphi}{dx} \tag{111}$$

When the electro-neutrality condition in the membrane is concerned (Eq. (89)), the differentiation of it with respect to the coordinate x will be equal to the multiplication of Eq. (111) with z_i and summation over all ions. When this operation is performed, the differential equation for the potential gradient was obtained as:

$$\frac{d\varphi}{dx} = \frac{\sum_{i=1}^{n} z_i \cdot v / D_{\text{ip}}(K_{\text{ic}} \cdot c_i - C_{\text{smp}})}{\frac{F}{R_g T} \cdot \sum_{i=1}^{n} z_i^2 \cdot c_i} \tag{112}$$

The solution of these equations system is performed iteratively applying the boundary conditions derived from the Donnan-steric partitioning Eq. (105).

4.4. Donnan steric pore model + Film model

Bowen and Mohammad [85] developed a model for the performance of the nanofiltration membrane in separating of a dye/salt solution. This model was developed based on the ENP and DSPM theoretical background (the same equations used as in 86, 89, 90, 91, 101, 103, 112) in which they incorporated the concentration polarization for a mixture of charged solute. This model was used to investigate the optimization of the processing condition in terms of the processing time, the membrane structure and the electrical properties were achieved.

The transport of organic solute through the membrane, in this case, they will neglect the electrostatic term in Eq. (86) the rejection can be written as:

$$R_j = 1 - \frac{C_{\text{sp}}}{C_{\text{smf}}} = 1 - \frac{K_{\text{ic}}\theta}{1 - \exp\left(-\text{Pe}\right)\left(1 - \vartheta K_{\text{ic}}\right)} \tag{113}$$

where the Péclet number Pe, is given as:

$$\text{Pe} = \frac{K_{\text{ic}}}{K_{\text{id}}} \cdot V \cdot \frac{\Delta x}{D_{\text{ib}} \cdot \varepsilon} \tag{114}$$

In the limiting case of Pe → ∞, the asymptotic rejection values will approach $(1 - \theta K_{\text{ic}})$. Thus, $(1 - \theta K_{\text{ic}})$ is a parameter that can be used to compare the limiting rejections of solute ions for various sizes. The Hagen–Poiseuille equation gives the relationship between the two terms the pure water flux and the applied pressure across the membrane:

$$J_w = r_p^2 \cdot \frac{\Delta P}{8 \cdot \mu\left(\frac{\delta}{\varepsilon}\right)} \tag{115}$$

If the concentration polarization close to the membrane surface was assumed to occur within a boundary film layer of thickness.

In the case of charged systems a mass balance for the film layer yields:

$$J_i = -D_{\text{ib}} \cdot \frac{dC_i}{dx} - z_i \cdot \frac{F}{R_g T} \cdot C_i \cdot D_{\text{ib}} \cdot \frac{d\varphi_f}{dx} + C_i \cdot J_V \tag{116}$$

This is similar to Eq. (86) except for the diffusivity here represents the bulk diffusivity in the solution. The net solute flux was written as in Eq. (103). This equation can be solved using the assumption of the boundary conditions: at $x = -\delta$, $c = C_{\text{ib}}$ and at $x = 0$, $c = C_{\text{iw}}$.

For a binary salt system, the cation and anion will move together due to the requirement of electro-neutrality. Eq. (116) can be solved for both ions and the flux expressed as:

$$J_c = J_a = -D_{\text{eff},b} \cdot \frac{dC_{\text{cation/anion}}}{dx} + C_{\text{cation/anion}} \cdot J_V \tag{117}$$

where $D_{\text{eff},\infty}$, depict the salts effective diffusivity ($\text{m}^2\ \text{s}^{-1}$):

$$D_{\text{eff},b} = D_{\text{cation}} \cdot D_{\text{anion}} \cdot \frac{(z_{\text{cation}} - z_{\text{anion}})}{z_{\text{cation}} \cdot D_{\text{cation}} - z_{\text{anion}} \cdot D_{\text{anion}}} \tag{118}$$

The boundary condition presented above can be used and the wall concentration C_{sm} can be replaced with other measurable terms as:

$$\frac{J_V}{k} = \ln \frac{C_{\text{sm}} - C_p}{C_{\text{smf}} - C_p} \tag{119}$$

The result is presented above can be applied also in the case of uncharged solute. Where k is defined as the coefficient of mass-transfer in the polarized boundary layer, but for a case of charged binary system was written as:

$$k = \frac{D_{\text{eff},b}}{\delta} \tag{120}$$

The correlation of the Sherwood number (Sh) was used to determine the mass-transfer coefficient as a function of Reynolds and Schmidt numbers as follows:

$$\mathrm{Sh} = k \cdot \frac{r}{D_{\mathrm{eff},b}} = s\left(\mathrm{Re}\right)^{n} \cdot \mathrm{Sc}^{0.33} \tag{121}$$

$$\mathrm{Re} = w \cdot \frac{r^2}{\upsilon} \tag{122}$$

$$\mathrm{Sc} = \frac{\mu}{D_{\mathrm{eff},b}} \tag{123}$$

In this case, the mass-transfer coefficient can be expressed as:

$$k = 0.23\left(\frac{r^2}{\upsilon}\right)^{0.567} \cdot \left(\frac{\upsilon}{D_{\mathrm{eff},b}}\right)^{0.33} \cdot \frac{D_{\mathrm{eff},b}}{r} \cdot w^{0.567} \tag{124}$$

In the diafiltration step, C_{sf} and C_{sp} respectively represent the bulk concentration of salt in the feed and permeate, thus a mass balance on salt in the system can be written as:

$$\frac{d\left(V_F C_{\mathrm{sf}}\right)}{dt} = -J_V \cdot S \cdot C_{\mathrm{sp}} \tag{125}$$

$$\frac{C_{\mathrm{sf}} dV_F}{dt} + \frac{V_F dC_{\mathrm{sf}}}{dt} = -J_V \cdot S \cdot C_{\mathrm{sp}} \tag{126}$$

Since the volume is constant, Eq. (126) can be written as:

$$\int_{t_{d0}}^{t_{d1}} dt = t_{d1} - t_{d0} = \int_{C_{\mathrm{sf}},t_{d0}}^{C_{\mathrm{sf}},t_{d1}} -\left(\frac{V_F}{J_V \cdot S}\right) \cdot \left(\frac{1}{C_{\mathrm{sp}} dC_{\mathrm{sf}}}\right) \tag{127}$$

The calculation of the necessary time for the diafiltration phase, we needed to integrate the right-hand term of Eq. (127). The final concentration of salt in the initial solution was given by $C_{\mathrm{sf,dt1}}$. Eq. (128) can be defined as on the observed rejection R:

$$\int_{t_{d0}}^{t_{d1}} dt = t_{d1} - t_{d0} = -\frac{V_F}{S} \int_{C_{\mathrm{sf}},t_{d0}}^{C_{\mathrm{sf}},t_{d1}} \frac{1}{\left(J_V \cdot C_{\mathrm{sf}} \cdot \left(1 - R\right)\right) dC_{\mathrm{sf}}} \tag{128}$$

Since the continuous change of the dye and salts throughout pre and post-concentration phases will get a complex concentration for that the mass balance for the dye gives:

$$\frac{d\left(V_F \cdot C_{\mathrm{dye},f}\right)}{dt} = 0 \tag{129}$$

Thus

$$\frac{C_{\mathrm{dye},f} \cdot dV_F}{dt} + \frac{V_F \cdot dC_{\mathrm{dye},f}}{dt} = 0 \tag{130}$$

While the dye was supposed to be eliminated in the feed, V_F was connected to the dye concentration and mass as:

$$V_F = \frac{M_{\mathrm{dye}}}{C_{\mathrm{dye},f}} \tag{131}$$

The change in V_F was connected to the membrane area and the permeate flux as we show in Eq. (132):

$$\frac{dV_F}{dt} = -S \cdot J_v \tag{132}$$

Substituting Eqs. (131) and (132) into Eq. (130) yields:

$$\frac{dC_{\mathrm{dye},f}}{dt} = S \cdot \frac{J_v}{M_{\mathrm{dye}}} C_{\mathrm{dye},f}^2 \tag{133}$$

Thus

$$\int_{t_{c0}}^{t_{c1}} dt = t_{c1} - t_{c0} = \frac{M_{\mathrm{dye}}}{S} \int_{C_{\mathrm{dye},f,t_{c0}}}^{C_{\mathrm{dye},f,t_{c1}}} \frac{1}{\left(J_v \cdot C_{\mathrm{dye},f}^2\right) dC_{\mathrm{dye},f}} \tag{134}$$

Eq. (134) was used to calculate the concentrating time for the dye solution from $C_{\mathrm{dye},f',\mathrm{tc0}}$ to $C_{\mathrm{dye},f,\mathrm{tcl}}$ which was related only with the dye concentrations and the permeate flux as:

$$\frac{dC_{\mathrm{sf}}}{dt} = S \cdot \frac{J_v}{M_{\mathrm{dye}}} C_{\mathrm{dye},f} \cdot C_{\mathrm{sf}} \cdot R \tag{135}$$

The change in salt concentration in the solution was calculated by dividing Eq. (135) by (134) as a function of dye concentration:

$$\ln\left(\frac{C_{\mathrm{dye},f,t_{c1}}}{C_{\mathrm{dye},f,t_{c0}}}\right) = \int_{C_{\mathrm{sf}} t_{c0}}^{C_{\mathrm{sf}} t_{c1}} \frac{1}{C_{\mathrm{sf}} \cdot R} dC_{\mathrm{sf}} \tag{136}$$

4.5. Hagmeyer and Gimbel model

Hagmeyer and Gimbel [86,87] developed a model for salts rejection within the nanofiltration membrane under the assumption of constant membrane potential in which they used zeta potential to calculate the surface charge of the nanofiltration membrane. Their model was based on two fundamental theory Nernst–Planck equation as indicated in Eq. (88) and Teorell–Meyer–Seiver (TMS) in terms of Donnan and Donnan dielectric partitions.

Hagmeyer and Gimbel [86] fitted their model using NaCl rejection measurements at neutral pH to determine the pore radius and the ratio of pore density and membrane thickness, in which they compared the calculation with rejection measurements for single salts and ternary ion mixtures at different pH values carried out for two fairly tight nanofiltration membranes (MWCO 150-300).

In Eq. (88) the convective coupling factor β_i was estimated by a center-line approximation for hindered particle motion in small pores for $\lambda \le 0.4$.

This approximation is equivalent to:

$$\beta_i = \left(1 - \lambda\right)^2 \cdot \left[2 - \left(1 - \lambda\right)^2\right] \cdot \left[\left(1 - \frac{2}{3} \cdot \lambda^2\right) - 0.163\lambda^3\right] \lambda \le 0.4 \tag{137}$$

The condition of electro-neutrality in the external solutions and the membrane was given as Eqs. (89) and (90), were used the Donnan equation for calculating the solute distribution at the solution-membrane interface as Eq. (101), the permeate concentration in nanofiltration was given by Eq. (104), we're using Eqs. (101) and (90) to Fig. 4 the concentration in both sides (feed/membrane).

We used the supposition that activity coefficient in the bulk and the pore phase is equal and they calculated the effective volume charge density in the pore using Eq. (138), taking into account an equal surface charge σ_c in the pore and the surface of the membrane:

$$X_M = 2\times\frac{\sigma_c}{r_p\cdot F} \tag{138}$$

The membrane effective surface charge density was estimated by the measurements of streaming potential to determine the zeta potential of the membrane and assuming that the electro-kinetic charge density at the shear plane is close to the effective charge density in the membrane; The electro-kinetic charge density depends on the zeta potential as:

$$\sigma_c = \left(2\cdot\varepsilon_0\cdot\varepsilon_b\cdot k_b\cdot T\cdot\sum_i C_i\cdot N_A\cdot\left[\exp\left(-z_i\cdot e\cdot\frac{\varsigma}{k_b\cdot T}\right)-1\right]\right)^{0.5} \tag{139}$$

The membrane flux was:

$$J_w = j_w\cdot\varepsilon \tag{140}$$

The integration of Eq. (88) across the membrane thickness and changing the pore volume flux by the membrane flux (Eq. (140)) in which were determined the ratio of ε/δ. This ratio can be expressed by using the pore radius and the pore density *n* as follows:

$$\frac{\varepsilon}{\delta} = n\cdot\pi\cdot\frac{r_p^{\,2}}{\delta} \tag{141}$$

Using the Helmholtz–Smoluchowski equation [88] to calculate the zeta potential according to this equation:

$$\varsigma = \Delta U\cdot\upsilon\cdot\frac{L}{\Delta P\cdot\varepsilon_r\cdot S\cdot R_g} \tag{142}$$

In the case of low zeta potential Eq. (139) was simplified as:

$$\sigma_c = \left(\varepsilon_0\cdot\phi_D\cdot\frac{e}{k_b\cdot T}\right)^{0.5}\cdot\varsigma\cdot\left(\sum_i C_i\cdot z_i^2\right)^{0.5} \tag{143}$$

Comparing the above equation for 1–1 electrolyte by using the Freundlich type isotherm in which the effective charge density was related to the equivalent concentration c_E:

$$\sigma_c = e\cdot c_E^s \tag{144}$$

The value of *s* depends on the membrane type.

Taking into account the change of dielectric constant between the bulk and the pores, an additional term will appear and Eq. (101) can be written as:

$$\frac{C_{\mathrm{sf}}}{C_{\mathrm{sm}}} = \exp\left(-z_i\cdot F\cdot\frac{\Delta\varphi}{R_g\cdot T}-\frac{\Delta W}{k_b\cdot T}\right) \tag{145}$$

If the bulk and the pore are an infinite medium of dielectric constants (ε_b,ε_p), then the change of electrostatic free energy was gotten according to the Born model [89] as:

$$\Delta W = z_i^2\cdot\frac{e^2}{8\pi\cdot\varepsilon_0\cdot r_s}\left(\frac{1}{\varepsilon_b}-\frac{1}{\varepsilon_p}\right) \tag{146}$$

where r_s is the ion radius (m).

It was shown by several authors that in narrow pores the induced energy by the dielectric of the membrane should be considered so that the change of the electrostatic free energy of an ion between the bulk and the membrane pore was written as:

$$\Delta W = z_i^2\cdot\frac{e^2}{8\pi\cdot\varepsilon_0\cdot r_s}\left(\frac{1}{\varepsilon_b}-\left(\frac{1}{\varepsilon_p}+\frac{\frac{0.393}{r_p}}{r_s\cdot\varepsilon_m}\left(1-\frac{\varepsilon_m}{\varepsilon_p}\right)^2\right)\right) \tag{147}$$

4.6. Afonso and De Pinho model [90]

Afonso and De Pinho [90], they described the transport of single salts solution of $MgSO_4$, $MgCl_2$, and Na_2SO_4 through an amphoteric nanofiltration membrane, in their work Afonso and De Pinho [90] was involving the extending Nernst–Planck equation and the Donnan equilibrium at the membrane-solution interface.

The concentration polarization is defined by the following relation:

$$\frac{C_{\mathrm{smf}}-C_{\mathrm{smp}}}{C_{\mathrm{if}-}C_{\mathrm{smp}}} = \exp\left(0.162\cdot\frac{\mathrm{Re}_p^{0.93}}{\mathrm{Re}^{0.29}}\cdot\mathrm{Sc}^{\frac{2}{3}}\right) \tag{148}$$

Reynolds numbers for the feed and the permeate was defined, as:

$$\mathrm{Re} = \rho_f\cdot\frac{D\langle v\rangle}{\upsilon_f(P\cdot 2)} \tag{149}$$

$$\mathrm{Re}_p = \rho_p\cdot D\cdot\frac{\upsilon_p}{\upsilon_p} \tag{150}$$

The osmotic pressure effect on the permeate flux was given by:

$$J = v_p\cdot\rho_p = A\left[\Delta P-\left(\pi_b\left(C_{\mathrm{smf}}\right)-\pi_p\left(C_{\mathrm{smp}}\right)\right)\right] \tag{151}$$

The continuity equation in rectangular coordinates is given in the case of steady-state unidirectional flow of an incompressible fluid:

$$v_M = \text{const} = v_p \tag{152}$$

A differential steady-state mass balance for solute *j* yields after integration:

$$J_{jy} = \text{const} = v_p \cdot C_{\text{smp}} \cdot \vartheta_j \tag{153}$$

The expression of the total flux of solute *j* given as the sum of three parameters (diffusion, convection and electro-migration) in which can be defined by the extended Nernst–Planck equations:

$$J_{\text{Cation},y} = -D_{\text{Cation},s} \cdot \frac{dC_{\text{cation}}}{dy} + v_M C_{\text{Cation}} - D_{\text{Cation},s} \cdot z_{\text{Cation}} \cdot \frac{F}{R_g T}\frac{d\phi}{dy} C_{\text{cation}} = v_p \cdot C_{\text{smp}} \cdot \vartheta_{\text{Cation}} \tag{154}$$

$$J_{\text{Anion},y} = -D_{\text{Anion},s} \cdot \frac{dC_{\text{Anion}}}{dy} + v_M C_{\text{Anion}} - D_{\text{Anion},s} \cdot z_{\text{Anion}} \cdot \frac{F}{R_g T}\frac{d\varphi}{dy} C_{\text{Anion}} = v_p \cdot C_{\text{smp}} \cdot \vartheta_{\text{Anion}} \tag{155}$$

The system of Eqs. (154) and (155) satisfies the condition of null electrical current flux:

$$z_{\text{Cation}} \cdot J_{\text{Cation},y} + z_{\text{Anion}} \cdot J_{\text{Anion},y} = v_p \cdot C_{\text{Sp}} \left(z_{\text{Cation}} \cdot \vartheta_{\text{Cation}} + z_{\text{Anion}} \vartheta_{\text{Anion}} \right) = 0 \tag{156}$$

In this case, the Donnan equilibrium is written as:

$$\left(\frac{\gamma_{\text{Anion},s}}{\gamma_{\text{Anion},m}} \right)^{z_{\text{Cation}}} = \left(\frac{\gamma_{\text{Cation},m}}{\gamma_{\text{Cation},s}} \right)^{-z_{\text{Anion}}} \tag{157}$$

The relations used for the electro-neutrality condition in the permeate and the membrane was given, as:

$$z_{\text{Cation}} \cdot C_{\text{cation},p} + z_{\text{Anion}} \cdot C_{\text{Anion},p} = 0 \tag{158}$$

$$z_{\text{Cation}} \cdot C_{\text{Cation},m} + z_{\text{Anion}} \cdot C_{\text{Anion},m} - c_i = 0 \tag{159}$$

where c_i is the effective charge concentration that exists in the membrane active layer.

4.6.1. In the case of feed-membrane interfaces

$MgSO_4$:

$$C_{\text{Cation},1} = \frac{c_i}{4} + \sqrt{\frac{c_i^2}{16} + C_{\text{smf}}^2} \tag{160}$$

$MgCl_2$:

$$C_{\text{Anion},1} = 2\frac{c_i}{3}\cos\left(60° - \frac{1}{3}\arccos\left(\frac{\left(\frac{c_i^3}{27}\right) - 4C_{\text{smf}}^3}{\left(\frac{c_i}{3}\right)^3} \right) \right) - \frac{c_i}{3} \tag{161}$$

Na_2SO_4:

$$C_{\text{Cation},1} = \sqrt[3]{a_1 + \sqrt{a_2}} + \sqrt[3]{a_1 - \sqrt{a_2}} + \frac{c_i}{3} \tag{162}$$

Here a_1 and a_2 represent:

$$a_1 = \frac{c_i^3}{27} + 4C_{\text{smf}}^3 \tag{163}$$

$$a_2 = \frac{8c_i^3 \cdot C_{\text{smf}}^3}{27} + 16C_{\text{smf}}^6 \tag{164}$$

4.6.2. In the case of permeate-pore interface

$MgSO_4$:

By involving the coefficients of the salts activity and the activity of the solute, associated with $C_{\text{Cation},p} = C_{\text{Anion},p} = C_{\text{smp}}$; and supposing that $\gamma_{\pm 2} = \gamma_{\pm p}$, was obtained:

$$C_{\text{smp}} = \sqrt{C_{\text{Cation},2} \cdot C_{\text{Anion},2}} \tag{165}$$

The interfacial expression for the Donnan equilibrium was written as:

$$(\gamma_{\text{Cation},2} \cdot \gamma_{\text{Anion},2})^2 = \left(\gamma_{\text{Cation},p} \cdot \gamma_{\text{Anion},p}\right)^2 \tag{166}$$

$MgCl_2$:

By involving the coefficients of the salts activity and the activity of the solute, associated with $C_{\text{Cation},p} = C_{\text{Anion},p}/2 = C_{\text{smp}}$; and supposing that $\gamma_{\pm 2} = \gamma_{\pm p}$, was obtained:

$$C_{\text{smp}} = \sqrt[3]{C_{\text{Anion},2}^2 \cdot \frac{C_{\text{Cation},2}}{4}} \tag{167}$$

The interfacial expression for the Donnan equilibrium was written as:

$$\left(\gamma_{\text{Cation},2} \cdot \gamma_{\text{Anion},2}\right)^2 = \left(\gamma_{\text{Cation},p} \cdot \gamma_{\text{Anion},p}\right)^2 \tag{168}$$

Na_2SO_4:

By involving the coefficients of the salts activity and the activity of the solute, associated with $C_{\text{Cation},p}/2 = C_{\text{Anion},p} = C_{\text{smp}}$; and supposing that $\gamma_{\pm 2} = \gamma_{\pm p}$, was obtained:

$$C_{\text{smp}} = \sqrt[3]{C_{\text{Cation},2}^2 \cdot \frac{C_{\text{Anion},2}}{4}} \tag{169}$$

The interfacial expression for the Donnan equilibrium was written as:

$$\left(\gamma_{\text{Anion},2}\cdot\gamma_{\text{Cation},2}\right)^2=\left(\gamma_{\text{Anion},p}\cdot\gamma_{\text{Cation},p}\right)^2 \tag{170}$$

4.7. Bowen and Welfoot model

In this work Bowen and Welfoot [54] provided a more rigorous description of the rejection of charged and uncharged solute based on the DSPM, in which Bowen and Welfoot [54] included the effects of pressure on chemical potential, and hence on solute transport, and of a pore radius dependent viscosity.

In this new contribution, Bowen and Welfoot [54] reduced the parameters of the variation of uncharged solute rejection with effective pressure driving force which depends on only one parameter (r_p) rather than two parameters (r_p and $\Delta x/\delta$), and for the charged solute the variation of ionic rejection with effective pressure driving force now being dependent on two parameters (r_p and X_M) rather than three parameters (r_p, $\Delta x/\delta$, and X_M) presented in the previous models DSPM; wherein they included in this model the effect of dielectric exclusion due to the changes in the properties of the solvent in the pores and the corresponding increase in the solute solvation energy.

Description of solvent velocities based on the Hagen–Poiseuille expression:

$$v=r_p^2\cdot\frac{\Delta P_e}{8\cdot\eta\cdot\delta} \tag{171}$$

where

$$\Delta P_e=\Delta P-\Delta\pi \tag{172}$$

4.7.1. Case of rejection uncharged solute

The hydro-dynamical model is frequently used to describe the transport for the uncharged solute, modified to incorporate the hindered convection and diffusion within the pores:

$$J_s=K_c\cdot c\cdot v-c\cdot\frac{D_p}{R_gT}\frac{d\mu}{dx} \tag{173}$$

The chemical potential, μ, for uncharged solute was written as:

$$\mu=R_gT\ln a+V_sP+\text{cst} \tag{174}$$

With a low solute concentration, the solution can be supposed to behave ideally preferably so that differentiation of Eq. (174) and substitution into Eq. (173) give:

$$J_s=K_c\cdot c\cdot v-c\cdot\frac{D_p}{R_gT}\cdot V_s\cdot\frac{dP}{dx}-D_p\frac{dc}{dx} \tag{175}$$

In the nanofiltration pore and for laminar flow, the pressure gradient was presented from the rearrangement of Hagen–Poiseuille expression in which the pressure gradient assumed to be constant along the pore so:

$$\frac{dP}{dx}=\frac{\Delta P_e}{\delta}=8.\eta.\frac{v}{r_p^2} \tag{176}$$

The expression for the concentration gradient was defined as:

$$\frac{dc}{dx}=\frac{v}{D_p}\cdot\left[\left(K_c-\frac{D_p}{R_gT}\cdot V_s\cdot\frac{8\cdot\eta}{r_p^2}\right)c-C_p\right] \tag{177}$$

After neglecting concentration polarization, this equation was integrated over the membrane thickness ($0 < x < \Delta x$) using the following boundary conditions:

$$C_{x=0}=\Phi\cdot C_f \text{ and } C_{x=\Delta x}=\Phi\cdot C_p \tag{178}$$

where Φ represents the coefficient of uncharged solute steric partitioning.

To simplify the solution was introduced y as a dimensional term which can be considered independent of solute concentration with the assumption that V_s and D_p are independent of concentration:

$$y=\frac{D_p}{R_gT}\cdot V_s\cdot\frac{8\cdot\eta}{r_p^2} \tag{179}$$

The concentration gradient will be integrated using the boundary conditions above yields:

$$\frac{C_p}{C_f}=\frac{\left[\{K_c-Y\}\Phi\right]\exp[\text{Pe}']}{\left[\{K_c-Y\}\Phi\right]-1+\exp[\text{Pe}']} \tag{180}$$

where the expression for the modified Péclet number, Pe′, was given as:

$$\text{Pe}'=\{K_c-Y\}\cdot v\cdot\frac{\delta}{D_p} \tag{181}$$

Eq. (180) can be substituted as the solute rejection definition, to writing as:

$$R=1-\frac{C_p}{C_f}=1-\frac{\left[\{K_c-Y\}\Phi\right]}{1-\left[1-\{K_c-Y\}\Phi\right]\exp[-\text{Pe}']} \tag{182}$$

The water velocity within the pore will be substituted using Eq. (171), redefine Pe′ as follows:

$$\text{Pe}'=r_p^2\cdot\frac{\{K_c-Y\}\Delta\text{Pe}}{8\cdot\eta\cdot D_p} \tag{183}$$

In their model they took a cylindrical nanofiltration pore that has an annulus with the thickness of one water molecule, which is represented an inner layer of adsorbed molecules, (d = 0.28 nm) having an increased viscosity ($\eta_{\text{layer}} = 10\eta_0$). We should note that the central part of the pore is supposed to have the same viscosity of bulk water, if we had an averaged viscosity in terms of area, the substitution of η_{layer} and rearrangement give:

$$\frac{\eta}{\eta_0} = 1 + 18\left(\frac{d}{r_p}\right) - 9\left(\frac{d}{r_p}\right)^2 \tag{184}$$

The diffusivity of the solutes will be affected by the change in viscosity, the pore diffusivity D_p must be redefined as follows:

$$D_p^* = D_p\frac{\eta_0}{\eta} = K_d \cdot D_\infty \cdot \frac{\eta_0}{\eta} \tag{185}$$

So the modified Péclet number can be rewritten as:

$$\text{Pe}' = r_p^2 \cdot \frac{\{K_c - Y\}\Delta\text{Pe}}{8 \cdot \eta \cdot D_p^*} = r_p^2 \cdot \frac{\{K_c - Y\}\Delta\text{Pe}}{8 \cdot \eta_0 \cdot K_d \cdot D_\infty} \tag{186}$$

4.7.2. Case of salts rejection

The transport equation was based on extended Nernst–Planck equation (Eq. (87)), the ionic flux of solute i was defined as follows:

$$J_i = K_{\text{ic}} \cdot c_i \cdot v - c_i \cdot \frac{D_{\text{ip}}}{R_g T}\frac{d\mu_i}{dx} \tag{187}$$

Electrochemical potential, μ_i, was defined as:

$$\mu_i = R_g T \ln a_i + V_i \cdot P + z_i \cdot F \cdot \varphi + \text{cst} \tag{188}$$

The standard assumption used to connect the solute activity to its concentration was an activity coefficient as we have shown ($a_i = \gamma_i c_i$). Manipulation used with Eqs. (188) and (187) give the transport equation as:

$$\begin{aligned} J_i = -c_i \cdot \frac{D_{\text{ip}} d\left[\ln\gamma_i\right]}{dx} - c_i \cdot D_{\text{ip}} \cdot \frac{V_i}{R_g T}\frac{dP}{dx} - \frac{D_{\text{ip}} dc_i}{dx} - \\ z_i \cdot c_i \cdot D_{\text{ip}} \cdot \frac{F}{R_g T}\frac{d\varphi}{dx} + K_{\text{ic}} \cdot c_i \cdot v \end{aligned} \tag{189}$$

This expression gives us the different transport mostly used in nanofiltration models; in this model, the solute flux was defined on a pore area basis and it was assumed to neglect the gradient of $\ln\gamma_i$ which implies that the concentration within the pore is very small. For dilute bulk electrolytes, the Debye–Hückel theory predicts that $\ln\gamma_i \infty \sqrt{I}$ [91]. However, were used the same theory to describe electrolytes within pores since the theory supposed that bulk solutions with equal numbers of cations and anions.

Substitution and rearrangement of Eqs. (103) and (179) into Eq. (189) allow the concentration gradient within the pore to be derived:

$$\frac{dc_i}{dx} = \frac{v}{D_{\text{ip}}} \cdot \{K_{\text{ic}} - Y_i\}c_i - C_{\text{smp}}] - z_i \cdot c_i \cdot \frac{F}{R_g T}\frac{d\varphi}{dx} \tag{190}$$

The electro-neutrality condition within the pore presented as Eq. (89), the external summation of the potential gradient (supposed to be equal for all ions) defined as:

$$\frac{d\varphi}{dx} = \frac{\sum_{i=1}^{n} z_i \cdot v / D_{\text{ip}}\left(\{K_{\text{ic}} - Y_i\}c_i - C_{\text{smp}}\right)}{\frac{F}{R_g T} \cdot \sum_{i=1}^{n} z_i^2 \cdot c_i} \tag{191}$$

The most commonly used partitioning equilibrium expression as Eq. (101), the orientation of the water molecule at the pore walls will similarly lead to a reduction in dielectric constant, which they supposed a high value of frequency limit in the layer ($\varepsilon^* \approx 6$). For more understanding, they supposed that the solvent crossing the pore will compose of one layer of the orientated water molecule and inner part having bulk dielectric proprieties, in which they have bulk dielectric properties in the internal part. Then were calculated the variation of average pore dielectric constant in geometric basis (supposing $\varepsilon_b = 80$ for a monovalent ion in water):

$$\varepsilon_p = 80 - 2\left(80 - \varepsilon^*\right)\left(\frac{d}{r_p}\right) + \left(80 - \varepsilon^*\right)\left(\frac{d}{r_p}\right)^2 \tag{192}$$

If we take into account the change of dielectric constant between the bulk and the pores an additional term called the solvation energy will appear and Eq. (101) is written as:

$$\frac{c_i}{C_{\text{smf}}} = \exp\left(-z_i \cdot F \cdot \left(\frac{\Delta\varphi_D}{R_g \cdot T}\right)\exp\left(\frac{-\Delta W_i}{k_b \cdot T}\right)\right) \tag{193}$$

The supported assumption in the experiment indicates that the salts rejection in the membrane iso-electric point cannot be only described by the exclusion steric, in which they present another rejection mechanism; the final form of partitioning expression used in their study was represented as:

$$\frac{c_i}{C_{\text{smf}}} = \theta_i \exp\left(-z_i \cdot F \cdot \left(\frac{\Delta\varphi_D}{R_g \cdot T}\right)\exp\left(\frac{-\Delta W_i}{k_b \cdot T}\right)\right) \tag{194}$$

where the solvation energy barrier was calculated from the Born model in which the Born energy gives the electrostatic free energy of an ion in the medium of dielectric constant [92], by using the molecular approach were found the expression of the solvation energy barrier presented as in Eq. (146).

For n solute and j data point of each solute then the least-squares fitting objective function (they used this parameter for comparison between the different solute) was written as follows:

$$S_y = \sqrt{\frac{\sum_1^n \sum_1^j \left(R_{\text{exp}} - R_{\text{calc}}\right)^2}{j_{n-1}}} \tag{195}$$

4.8. Linearized model

To simplifies the solution of nanofiltration transfer phenomena for electrolyte rejection, a finite-difference linearization of pore concentration gradient was provided to simplify the solution of three parameters model (pore radius, membrane charge, pore dielectric constant) described in the previous model; Bowen et al. [93] proposed a linearized model in which they introduce the dielectric exclusion effect to reduces the magnitude of predicted values of X_M and changes the emphasis from X_M to pore radius through pore dielectric constant as the dominant parameter [93]; this model used for reducing the systems of 1-ODE to algebraic equation by eliminating most of the numerical integration. The advantage of this model over-analytical model is highlighted when the calculations made for mixtures solute systems.

4.8.1. Rejection of 1-1 electrolyte using linearization

In the case of all single electrolyte such as NaCl, KCl …, we propose $C_{1,\mathrm{wl}} = C_{2,\mathrm{wl}} = C_{\mathrm{wl}}$, $C_{1,p} = C_{2,p} = C_p$, $z_1 = -z_2 = 1$, so the equation of the potential gradient will written as follows:

$$\frac{F}{R_gT}\frac{d\varphi}{dx} = \frac{\left[\begin{array}{l} \left(K_{1,c}\cdot\frac{v}{D_{1,p}} - K_{2,c}\cdot\frac{v}{D_{2,p}}\right)c_1 - \left(\frac{v}{D_{1,p}} - \frac{v}{D_{2,p}}\right) \\ C_p - \left(K_{2,c}\cdot\frac{v}{D_{2,p}}\right)X_M \end{array}\right]}{2c_1 + X_M} \tag{196}$$

The concentration gradient (Eq. (111)) was presented as:

$$\frac{dc_1}{dx} = \frac{\left\{\begin{array}{l} \left(K_{1,c}\cdot\frac{v}{D_{1,p}} + K_{2,c}\cdot\frac{v}{D_{2,p}}\right)c_1^2 + \left[\begin{array}{l} \left(K_{1,c}\cdot\frac{v}{D_{1,p}} + K_{2,c}\cdot\frac{v}{D_{2,p}}\right) \\ X_M - \left(\frac{v}{D_{1,p}} + \frac{v}{D_{2,p}}\right)C_p \end{array}\right] \\ c_1 - \frac{v}{D_{1,p}}\cdot X_M\cdot C_p \end{array}\right\}}{2c_1 + X_M} \tag{197}$$

The concentration gradient will be effectively constant and hence the concentration profiles linear provided the effect of the c^2 term is relatively small. Under these conditions, the concentration gradient can be approximated as follows:

$$\frac{\Delta c_1}{\delta} = \frac{\left\{\begin{array}{l} \left(K_{1,c}\cdot\frac{v}{D_{1,p}} + K_{2,c}\cdot\frac{v}{D_{2,p}}\right)c_1^{\mathrm{av}2} + \left[\begin{array}{l} \left(K_{1,c}\cdot\frac{v}{D_{1,p}} + K_{2,c}\cdot\frac{v}{D_{2,p}}\right) \\ X_M - \left(\frac{v}{D_{1,p}} + \frac{v}{D_{2,p}}\right)C_p \end{array}\right] \\ c_1^{\mathrm{av}} - \frac{v}{D_{1,p}}\cdot X_M\cdot C_p \end{array}\right\}}{2c_1^{\mathrm{av}} + X_M} \tag{198}$$

where

$$\frac{dc_1}{dx} = \frac{\Delta c_1}{\delta} = \frac{c_{1\mathrm{sp}} - c_{1\mathrm{sm}}}{\delta}, c_1^{\mathrm{av}} = \frac{c_{1\mathrm{sp}} + c_{1\mathrm{sm}}}{2} \tag{199}$$

Inclusion of Eq. (200) in Eq. (199) and rearrangement yields to the following explicit expression for C_p:

$$\mathrm{Pe} = \frac{\{K_c v\cdot\delta\}\Delta\mathrm{Pe}}{D_{i,p}} = r_p^2\cdot\frac{\{K_{i,c}\}\Delta\mathrm{Pe}}{8\cdot\eta\cdot D_{i,p}} \tag{200}$$

$$C_p = \frac{\left\{\begin{array}{l} \left(\mathrm{Pe}_1 + \mathrm{Pe}_2\right)c_1^{\mathrm{av}2} + \left(\mathrm{Pe}_1 + \mathrm{Pe}_2\right)\cdot X_M\cdot c_1^{\mathrm{av}} \\ -\left(2c_1^{\mathrm{av}} + X_M\right)\cdot\Delta c_1 \end{array}\right\}}{\left(\frac{\mathrm{Pe}_1}{K_{1,c}} + \frac{\mathrm{Pe}_2}{K_{2,c}}\right)\cdot c_1^{\mathrm{av}} + \frac{\mathrm{Pe}_1}{K_{1,c}}\cdot X_M} \tag{201}$$

The Donnan potential at the pore inlet is the same for both solutes (although it differs from the potential at the pore outlet). Rearrangement and incorporation of partial partition coefficient θ_i in Eq. (194) gives:

$$\Delta\varphi_D(0) = -\frac{R_gT}{F}\cdot\left[\ln\left(\frac{c_{\mathrm{sm1}}}{\theta_1\cdot C_{\mathrm{wl}}}\right)\right] = \frac{R_gT}{F}\cdot\left[\ln\left(\frac{c_{\mathrm{sm2}}}{\theta_2\cdot C_{\mathrm{wl}}}\right)\right] \tag{202}$$

The concentrations of ion 2, c_2, and $C_{2,p}$, can be eliminated, by using the electro-neutrality conditions within the pore and the permeate solutions, by definition:

$$c_2 = \frac{(z_1c_1 + X_M)}{-z_2}, C_{2,p} = -\frac{z_1}{z_2}C_{1,p} \tag{203}$$

Algebraic manipulation of Eq. (202) with Eq. (203) results in a quadratic expression which defined partitioning, so the solution can be written as:

$$c_{\mathrm{sm1}} = \frac{-X_M + \sqrt{X_M^2 + 4\theta_1\theta_2C_{\mathrm{wl}}^2}}{2} \tag{204}$$

$$c_{\mathrm{sp1}} = \frac{-X_M + \sqrt{X_M^2 + 4\theta_1\theta_2C_p^2}}{2} \tag{205}$$

For the case of three ions rejection, Bowen et al. [93] was examined the system contain ($\mathrm{Na^+}$:$\mathrm{SO_4^{2-}}$:$\mathrm{Cl^-}$, $\mathrm{Cl^-}$:$\mathrm{Mg^{2+}}$:$\mathrm{Na^+}$), the detailed model will be found it in the appendix of his presented work [93], the ion valences of this mixture system are +1:–2:–1 and –1:+2:+1, respectively.

After many rearrangements used in this order of valence yields to the cubic equation in the pore inlet and outlet as follows:

$$z_1c_{\mathrm{sm1}}^3 + X_Mc_{\mathrm{sm1}}^2 + z_3\theta_1\theta_3\cdot C_{3,\mathrm{wl}}\cdot C_{1,\mathrm{wl}}c_{\mathrm{sm1}} + z_2\theta_1^2\theta_2\cdot C_{2,\mathrm{wl}}\cdot C_{1,\mathrm{wl}}^2 = 0 \tag{206}$$

$$z_1c_{\mathrm{sp1}}^3 + X_Mc_{\mathrm{sp1}}^2 + z_3\theta_1\theta_3\cdot C_{3,p}\cdot C_{1,p}c_{\mathrm{sp1}} + z_2\theta_1^2\theta_2\cdot C_{2,p}\cdot C_{1,p}^2 = 0 \tag{207}$$

Solution of Eqs. (206) and (207) by using the Newton–Raphson method shows that there is only one real root to each equation [93].

4.9. Lefebvre et al. model (Hindred electro-transport theory)

Lefebvre et al. [94,95] implemented a new approach for describing nanoscale solute transport by using two nanofiltration membranes (loose ceramic TiO_2 and tighter organic nano filter) to study the rejection of single salts and multi-ions mixture. Their model was based on the hybrid hindered electro-transport theory (HETT) in which it is taken into account (ion charge and size including the hindrance factors of steric and hydrodynamic) in the extended Nernst–Planck equation and the Stokes equation; in their study, Lefebvre et al. used a simulator for solving the different numerical equations this latter called NANOFLUX.

In ceramic membranes it possible to measure the electrophoresis mobility u_E by using the assumption of double thin-film theory (Eq. (208)) with low zeta potential (Eq. (209)), then were used the classical equation of Helmholtz–Smoluchowski [88] (Eq. (210)), as follows:

$$\lambda_D = \left(\varepsilon \cdot \frac{R_g T}{2 \cdot F^2 \cdot I}\right)^{\frac{1}{2}} \ll r_{\text{agg}} \tag{208}$$

where r_{agg} was ceramic powder particle radius:

$$z_1 \cdot F \cdot \frac{\varsigma}{R_g T} < 2 \tag{209}$$

$$u_E \approx \frac{\varepsilon^* \cdot \varsigma}{\eta} \tag{210}$$

Hence, the membrane charge density was given as:

$$X_M = 0.30 \cdot u_E \cdot \frac{\sqrt{I}}{r_H} \tag{211}$$

In their work they supposed that the ENP equation was defined as:

$$j_i = -D_{\text{ip}} \cdot dc_{i(x)}^{\text{ave}} - z_i \cdot D_{\text{ip}} dc_{i(x)}^{\text{ave}} \cdot \tilde{\varphi} + K_{i,c} \cdot c_{i(x)}^{\text{ave}} \cdot j_v - D_{\text{ip}} dc_{i(x)}^{\text{ave}} \cdot \left(\ln \overline{\gamma}_l\right) \tag{212}$$

where

$$D_{\text{ip}} = K_{i,d} \cdot D_{\text{ib}} \cdot \frac{\delta}{\delta_{\text{eff}}} \tag{213}$$

And the activity coefficient can be written as:

$$\gamma_{\text{im}} = (\theta_i)^{-1} = \left(1 - \frac{r_i}{r_p}\right)^{-2} \tag{214}$$

The potential gradient is given as:

$$\partial_x \cdot \varphi^* = \frac{\sum_{i=1}^{2} - z_i \cdot D_{\text{ip}} dc_{i(x)}^{\text{ave}} + z_i \cdot K_{i,c} \cdot c_{i(x)}^{\text{ave}} \cdot j_v}{\sum_{i=1}^{2} z_i^2 \cdot D_{\text{ip}} \cdot c_{i(x)}^{\text{ave}}} \tag{215}$$

After using the electro-neutrality condition (Eq. (89)) yields to:

$$dc_{i(x)}^{\text{ave}} = -\frac{z_2}{z_1} dc_{2,x}^{\text{ave}} \tag{216}$$

Eq. (215) was substituted in Eq. (212) with including the membrane electro-neutrality conditions (Eqs. (89), (93), and (216)), were obtained the expression of Péclet number as follows:

$$\text{Pe} = J_v \cdot \frac{\delta}{D_{\text{pm}} \cdot \omega} = \frac{D_{s,p}}{D_{\text{pm}}} \int_{k_2^f}^{Tk2^p} \frac{y_2 + \alpha}{y_2^2 + \beta(T) y_2 + \gamma(T)} dy_2 \tag{217}$$

where

$$y_2 = \frac{c_2^{\text{ave}}}{c_2^f}, \beta = \widehat{\xi_f} - \frac{T}{\omega}; \alpha = \frac{|z_1|}{|z_1| + |z_2|}; \gamma = -T \cdot \frac{\overline{t_1} \cdot \widehat{\xi_f}}{\omega} \cdot \widehat{\xi_f};$$
$$\omega = K_{2,c} \cdot \overline{t_1} + K_{1,c} \cdot \overline{t_2}; D_{\text{pm}} = \max\left(\overline{D_1} \cdot \overline{D_2}\right);$$
$$D_{s,p} = D_1 \cdot D_2 \frac{\left(|z_1| + |z_2|\right)}{|z_1| \cdot D_1 + |z_2| \cdot D_2}$$

The integration of Eq. (217) was given as:

$$\text{Pe} = \frac{D_{s,p}}{\omega \cdot 2D_{\text{pm}}} = \begin{bmatrix} \ln\left(\frac{g\left(TK_{2p}\right)}{g\left(K_{2f}\right)}\right) + \frac{\widehat{\xi_f}\left(\frac{1-\tau}{1+\tau}\right) + \frac{T}{\omega}}{\sqrt{q(T)}} \\ \ln\left(g'\left(TK_{2p}\right) - \sqrt{q(T)}\right) \left(\frac{g'\left(K_{2p}\right) + \frac{\sqrt{q(T)}}{g'\left(TK_{2p}\right)} +}{\sqrt{q(T)}}\right) \\ \left(g'\left(K_{2p}\right) - \sqrt{q(T)}\right) \\ \\ \end{bmatrix} \tag{218}$$

While

$$q(T) = \widehat{\xi_f}^2 + \left(\frac{T}{\omega}\right)^2 - \left(\frac{2T\widehat{\xi_f}}{\omega}\right)\left(1 - 2\overline{t_1}\right);$$
$$\widehat{\xi_f} = \frac{|X_M|}{\upsilon_1 \cdot |z_1| \cdot c^f} = \frac{|\xi|}{\upsilon_1} \cdot |z_1|; \overline{t_1} = |z_1| \cdot \frac{\overline{D_1}}{|z_1| \cdot \overline{D_1} + |z_2| \cdot \overline{D_2}};$$
$$\delta_{\text{eff}} = \delta \cdot \frac{\tau}{\varphi_p}; K_{2p} = c_2^{\text{ave}} \cdot \frac{\delta}{T \cdot c_2^f}; K_{2f} = \frac{c_{\text{sm},2}^{\text{ave}}}{c_2^f};$$

With g, g' and q are respectively defined as:

$$g(x) = x^2 + b(T)x + a(T), g'(x) = 2 \cdot x + b(T),$$
$$q(T) = \left(\widehat{\xi_f}\right)^2 + T^2 - 2T \cdot \widehat{\xi_f}\left(1 - 2\overline{t_1}\right) \quad .$$

Finally

$$a = -T \cdot \widehat{\xi_f} \cdot \overline{t_1}, b = \widehat{\xi_f} - T$$

To obtain the limit transmission rate, Eq. (212) was used at the feed/membrane interface (C_{sm}) for the co-ion ($i = 2$) after neglected the diffusive contributions for high fluxes.

$$j_2 = -z_2 \cdot c_{\text{sm},2}^{\text{ave}} \cdot D_{2p} \cdot d\tilde{\theta} + K_{2,c} \cdot c_{\text{sm},2}^{\text{ave}} j_v = c_{p2} \cdot j_v \tag{219}$$

In this case, the potential gradient will be written as:

$$d\tilde{\theta} \approx \frac{\sum_{i=1}^{2} z_i \cdot K_{i,c} \cdot c_{\text{sm},i}^{\text{ave}} \cdot j_v}{\sum_{i=1}^{2} z_i^2 \cdot D_{\text{ip}} \cdot c_{\text{sm},i}^{\text{ave}}} \tag{220}$$

Then T_{lim} was found after using the electro-neutrality equation normalized by $c_{f,2}$ as Eq. (221) shows:

$$T_{\text{lim}} = K_{2f} \left(K_{2,c} + \frac{\overline{t_2} K_{2f} \left(K_{1,c} - K_{2,c} \right) + K_{1,c} \cdot \widehat{\xi_f}}{K_{2f} + \overline{t_1} \cdot \widehat{\xi_f}} \right) \tag{221}$$

Finally the rejection rate was defined as:

$$R = 1 - T_{\text{lim}} \tag{222}$$

4.10. Bandini and Vezzani model (Donnan-steric-dielectric exclusion model)

Bandini and Vezzani [96,97] proposed a general model to describe nanofiltration membrane performance in the separation of an aqueous solution containing electrolyte; this model presents an extension of DSPM in which they assumed that:

- The membrane is considered a charged porous layer and is characterized using three adjustable parameters such as average pore radius, volumetric charge density, and effective membrane thickness;
- Partitioning effects are described through steric hindrance and the Donnan equilibrium;
- Mass transfer through the membrane is based on the extended Nernst–Planck equation.

This model called DSPM and dielectric exclusion (DE) which took into account the dielectric constant differences between aqueous solution in the pore and the membrane material, the latter causes an electrostatic interaction between the ions of the solution and the polarization charge induced by the ions themselves.

The determination of the rejection mechanism which is related to dielectric effect was supposed by the role of the difference existing between both dielectric constants (the aqueous solution in the pores and the membrane material), to validate this model Bandini and Vezzani using a negatively charged membrane and the same parameters used as in the case of DSPM model for implemented their model (Nernst–Planck equation, electro-neutrality conditions in the both side, potential gradient, steric partition and membrane charge density), were cited the governing equations related to this model as follows:

The ion partition is defined as:

$$\frac{c_i}{C_{\text{smf}}} = \theta_i \cdot \exp\left(-z_i \cdot \frac{F}{R_g T} \cdot \Delta\varphi_D \right) \cdot \exp\left(-z_i^2 \cdot \Delta W_{i,\text{mp}} \right) \tag{223}$$

where

$$\Delta W_{i,\text{mp}} = r_B \cdot \left(\nabla_{DB} - \nabla_{DM} - \frac{1}{r_p} \cdot \ln\left(1 - h \cdot \exp\left(-2 \cdot r_p \cdot \nabla_{DM} \right) \right) \right) \tag{224}$$

In which r_B and γ are defined as:

$$r_B = \frac{F^2}{8\pi \cdot \varepsilon^* \cdot R_g \cdot T \cdot N_a}, h = \frac{\left(1 - \frac{\varepsilon_M}{\varepsilon^*} \right)}{\left(1 + \frac{\varepsilon_M}{\varepsilon^*} \right)}, \nabla_{DB} = \frac{\frac{1}{F}\sqrt{\varepsilon_b \cdot R_g T}}{\sqrt{2 I_B}},$$

$$\nabla_{DM} = \frac{\frac{1}{F}\sqrt{\varepsilon_p \cdot R_g T}}{\sqrt{2 I_M}}, I = \frac{1}{2} \cdot \sum_{i=1}^{n} z_i^2 c_i,$$

In the calculations, it was assumed that the dielectric constant of the solution in the pore (ε^*) is equal to its dielectric constant in the bulk (ε_b) and as the most of the nanofiltration polymeric membranes have dielectric constants in the range of 3–5, the membrane dielectric constant (ε_m) was taken as equal to 3 and ε_b was assumed close to the pure water value at room temperature so $\varepsilon_m/\varepsilon_b = 3/80$).

In the case of charged membranes, it can be reasonably supposed that the counter-ions concentration inside the membrane is remarkably higher than the co-ions concentration; for the case of single symmetric electrolyte (NaCl) and negatively charged membrane, we obtain the following equation:

$$z_1 \cdot c_1 \gg \left| z_2 \right| \cdot c_2 = X_M \tag{225}$$

So the rejection rate will define as:

$$R = 1 - \frac{K_{2\text{eff}}}{2\left(r_0 + \frac{1 - \Lambda}{G - 1} \right)} \left[\sqrt{\frac{X_M^2}{z_1^2 \cdot c_{\text{smf},1}^2} + 4\theta_1\theta_2 \exp\left(-2z_1^2 \cdot \Delta W_0 \right)} + \frac{X_M}{\left(z_1 \cdot c_{\text{smf},1} \right)} \right] \tag{226}$$

In which,

$$\Lambda = \frac{\frac{\overline{K}}{G - 1}\left(r_0 + \frac{1}{G - 1} \right) + \frac{r_0 - 1}{2} - \sqrt{\frac{\left(r_0 - 1 \right)^2}{4} + r_0 \left(r_0 + \frac{1}{G - 1} \right)\left(1 + \frac{1}{G - 1} \right) \cdot \overline{K}}}{\frac{\overline{K}}{\left(G - 1 \right)^2} - 1},$$

$$r_0 = \frac{c_{i,2}}{c_{i,1}}, G = \exp\left(K_{2\text{eff}} \cdot \frac{J_v}{D_{2p}} \delta \right),$$

$$\overline{K} = \exp\left(-2z_1^2 \cdot \Delta W_{i,\text{mp}} \right)\left(K_{2\text{eff}} \right)^2 \theta_1\theta_2$$

4.11. Aleman and Dickson model

Aleman and Dickson [98] performed one-dimensional mathematical model to predict the performances of commercial nanofiltration membrane in case of multi-ions electrolyte solution, in which Aleman and Dickson established their model according to three basic theory: ENP equation, Donnan equilibrium and Gouy–Chapman theory; Aleman and Dickson implemented their model based on several assumptions:

- The membrane is macroscopically uniform in thickness and is porous in nature.
- The pores are modeled as uniform capillaries that extend throughout the membrane with an evenly distributed throughout the surface of the membrane (cross-section).
- Entrance and exit effects are ignored since the membrane thickness is large compared to the pore radius (×1000).
- There is an equilibrium between the two sides of the membrane.
- Uniform distributions of charge density and mobile species within the pore; and dilute solution theory was applied in their implementation.

In their model Aleman and Dickson [98] introduce the Gouy–Chapman equation for the case of membrane charge calculation in somehow they treat the ions as point of charge taking into account the supposition of existence an electrostatic ionic adsorption which isn't limited to low potentials as in the Debye–Hückel, and they used the same approaches as in DSPM model.

The surface potential in the dimensionless form was defined as:

$$y^d = \varnothing \cdot \frac{F}{R_g T} \tag{227}$$

For cylindrical pore geometry the expression of volumetric charge density was related to surface charge density and pore radius, this latter was given as Eq. (228):

$$X_{\mathrm{VM}} = 2 \cdot \frac{\sigma_c}{r_p \cdot F} \tag{228}$$

Using the solution of the Gouy–Chapman equation for mixed electrolyte solutions for a flat surface, the surface charge density is related to the surface electrical potential and the feed electrolyte concentration by:

$$\sigma_c = \left(\frac{y^d}{\left|y^d\right|}\right)\sqrt{2 \cdot \varepsilon^0 \cdot \varepsilon^* \cdot R_g T}\left[\frac{\sum C_{\mathrm{smf}}\left(\begin{array}{l}\in_{i,+} \cdot \exp^{-z_{i,+y^d}} + \\ \in_{i,-} \cdot \exp^{-z_{i,-y^d}}\end{array}\right) -}{\sum C_{\mathrm{smf}} \cdot \left(\in_{i,+} + \in_{i,-}\right)}\right]^{1/2} \tag{229}$$

where ε^0, ε^*, ε_i respectively represent the dielectric constant of a vacuum, the relative dielectric constant of water, and the ion stochiometric coefficient. However, in this case, the pore surface cannot be considered flat.

For cylindrical coordinates, the analytical solution was only available for the case of single electrolytes as:

$$\sigma_c = -2 \cdot F \cdot \frac{C_{\mathrm{smf}} z_+}{\nabla}\left[2\sinh\left(\frac{z_+ \cdot y^d}{2}\right) + 2\tanh\left(\frac{\frac{z_+ \cdot y^d}{2}}{r_p \cdot \nabla}\right)\right] \tag{230}$$

where C_{smf} corresponds to the equivalent concentration of counter-ion in the feed solution and z_+ represents the valence of the counter-ion.

4.12. Szymczyk and Fievet model (Steric electric and dielectric exclusion model)

In this model, Szymczyk and Fievet [99] give a new contribution to describe the transport within a nanofiltration membrane for both geometry (cylindrical and slit-like) pore in which were included the dielectric exclusion in terms of both (Born effect and image forces).

The image forces were defined as the interactions with polarized interfaces this latter acting on an electric charge located near an infinite plane interface [100].

The steric, electric and dielectric exclusion model (SEDE) can be used to measure the rejection rate of the membrane and dielectric constant of the solution, with only adjustable parameter that taking into account the filling pores.

In the liquid phase the electrochemical potential of solute i ($\tilde{u}_i$) with valence z_i was written as:

$$\widetilde{u}_i = u_i^0 + k_b \cdot T \cdot \ln\left(\frac{c_i}{c_0}\right) + z_i \cdot e \cdot \varphi + W_i \tag{231}$$

They were assumed as the same local thermodynamic equilibrium between the two phases membrane/solution interface and bulk solution ($\tilde{u}_i^m = \tilde{u}_i^b$) so:

$$K_s = \exp\left(-\frac{z_i \cdot e \cdot \Delta\varphi + \Delta W_i}{k_b \cdot T}\right) \tag{232}$$

where K_s the distribution coefficient of i was defined as:

$$K_s = \frac{c_{\mathrm{smp}}}{c_{\mathrm{smf}}} \tag{233}$$

In this model they consider that ΔW_i (total interaction energy) given as the sum of four terms as follows:

$$\Delta W_i = -k_b \cdot T \ln \theta_i + \Delta W_{i,\mathrm{Born}} + \Delta W_{i,\mathrm{im}} + k_b \cdot T \ln\left(\frac{\gamma_{\mathrm{im}}}{\gamma_{\mathrm{ib}}}\right) \tag{234}$$

The above relation represents the sum of multi-terms in which the first one denotes the steric exclusion defined with the steric partitioning coefficient θ_i; the two other terms indicate the energy interaction due to the Born dielectric and image forces $\Delta W_{i,\mathrm{Born}}$ and $\Delta W_{i,\mathrm{im}}$ effects and the last one representing the difference of activity coefficient (γ_i) between the two side of the pore. Wherein the Debye–Hückel theory was used the extended law to calculate the activity coefficient (γ_i) as shown in Eq. (235):

$$\log\gamma_i = -B\cdot z_i^2\cdot\frac{\sqrt{I}}{1+\left(A\cdot r_i\cdot\sqrt{I}\right)} \tag{235}$$

With,

$$A = F\sqrt{\frac{2}{\varepsilon_0\cdot\varepsilon_r\cdot R_g\cdot T}}, B = e^2\cdot\frac{F}{\sqrt{2}\cdot 4\cdot \ln 10(\varepsilon_0\cdot\varepsilon_r\cdot R_g\cdot T)^{3/2}},$$

$$I = \frac{1}{2}\sum c_i\cdot z_i^2$$

where A, B, I are parameters used in this model.

Scaling ΔW_i on $k\cdot T$, Eq. (232) can be rewritten as:

$$K_s = \theta_i\cdot\frac{\gamma_{\text{ib}}}{\gamma_{\text{im}}}\cdot\exp\left(-z_i\cdot\Delta\varphi_D\right)\exp\left(-\Delta W'_{i,\text{Born}}\right)\exp\left(-\Delta W'_{i,\text{im}}\right) \tag{236}$$

While the prime symbol indicates that both $\Delta W'_{i,\text{Born}}$ and $\Delta W'_{i,\text{im}}$ are scaled on $k_b\cdot T$ and the expression of the normalized potential of Donnan given as $\Delta\varphi_D = (e/k_b\cdot T)\Delta\varphi$) involved in the mechanism of electrical exclusion. The work of charge transfer from a medium with the dielectric constant ε_b to a medium with the dielectric constant ε_p was given by:

$$\Delta W'_{i,\text{Born}} = \frac{\left(z_i\cdot e\right)^2}{8\cdot\pi\cdot\varepsilon_0\cdot k_b\cdot T\cdot r_{i,\text{cav}}}\left(\frac{1}{\varepsilon_p}-\frac{1}{\varepsilon_b}\right) \tag{237}$$

where ε_p, ε_b, respectively was given as the solution dielectric constant, inside pores and in the external bulk solution. The difference between this one and the one of Born model is that were used here the radius of the cavity formed by the solute i in water ($r_{i,\text{cav}}$) this latter can be defined as the distance from the center of the ion and the point where the dielectric constant becomes different from that of the vacuum.

In which the interaction energy equation due to the image force in the cylindrical and slit-like geometries was written as follows:

$$\Delta W'_{i,\text{im}} = 2\cdot\frac{\alpha_i}{\pi}\int_0^\infty\frac{\left[K_0(k)\cdot K_1(\upsilon)-\tilde{\beta}(k)\cdot K_0(\upsilon)\cdot K_1(k)\right]}{\left[I_1(\upsilon)\cdot K_0(k)+\tilde{\beta}(k)\cdot I_0(\upsilon)\cdot K_1(k)\right]} \tag{238}$$

dk for cylindrical pore

$$\Delta W'_{i,\text{im}} = -\alpha_i\ln\left[1-\left(\frac{\varepsilon_p-\varepsilon_m}{\varepsilon_p+\varepsilon_m}\right)\exp(-2u)\right]\text{forslit}-\text{likepore} \tag{239}$$

where ε_m is the constant dielectric for the membrane, I_0, I_1, K_0, K_1 are respectively the modified Bessel functions, k was the wave vector and hence:

$$\alpha_i = \frac{\left(z_i\cdot F\right)^2}{8\cdot\pi\cdot\varepsilon_0\cdot\varepsilon_p\cdot R_g\cdot T\cdot N_A\cdot r_p}, \upsilon = \sqrt{u^2+k^2},$$

$$\tilde{\beta} = \frac{k}{\sqrt{u^2+k^2}}\left(\frac{\varepsilon_p-\varepsilon_m}{\varepsilon_p+\varepsilon_m}\right),$$

$$u = \kappa_b\cdot r_p\sqrt{\sum_{\text{i}}\frac{z_i^2 c_i^b\cdot\theta_i\cdot\left(\dfrac{\gamma_i^m}{\gamma_i^b}\right)\exp\left(-z_i\cdot\Delta\varphi-\Delta W'_{i,\text{Born}}-\Delta W'_{i,\text{im}}\right)}{2\cdot I}},$$

$$\kappa_b = \left(\varepsilon_0\cdot\varepsilon_b\cdot R_g\cdot\frac{T}{2\cdot F^2\cdot I^b}\right)^{-\frac{1}{2}}$$

While N_A, r_p, respectively was the Avogadro number and the pore size, that is, for a cylindrical pore was used as radius and for a slit-like pore, we took it as the half-width.

For the case of the electro-neutrality equation were used the same as above, by the substitution of the electro-neutrality equation inside the pore and Eq. (236) were found that the electro-neutrality equations take the form:

$$\sum_i\left[z_i\cdot c_i^b\cdot\theta_i\cdot\frac{\gamma_{\text{ib}}}{\gamma_{\text{im}}}\cdot\exp\left(-z_i\cdot\Delta\varphi-\Delta W'_{i,\text{Born}}-\Delta W'_{i,m}\right)\right]+X_M = 0 \tag{240}$$

In this model, Szymczyk and Fievet [99] used the same extended Nernst–Planck equation as it's frequently form but the only difference are in the hindrance factor for the two geometry (cylindrical and slit-like pores); in the case of cylindrical geometry pore, were took the assumption of equations for $0 \le \lambda_i < 1$ as:

$$K_{\text{id}} = \frac{6\pi}{K_{i,t}} \tag{241}$$

$$K_{i,c} = \left(2-\theta_i\right)\cdot\frac{K_{i,s}}{2\cdot K_{i,t}} \tag{242}$$

where $K_{i,t}$ and $K_{i,s}$ defined as modified hindrance coefficient for diffusion and convection was given as:

$$K_{i,t} = \frac{9}{4}\cdot\pi^2\cdot\sqrt{2}\left(1-\lambda_i\right)^{-\frac{5}{2}}\left[1+\sum_{n=2}^{2}a_n\cdot\left(1-\lambda_i\right)^n\right]+\sum_{n=0}^{4}a_n+3\lambda^n \tag{243}$$

$$K_{i,s} = \frac{9}{4}\cdot\pi^2\cdot\sqrt{2}\left(1-\lambda_i\right)^{-\frac{5}{2}}\left[1+\sum_{n=2}^{2}b_n\cdot\left(1-\lambda_i\right)^n\right]+\sum_{n=0}^{4}b_n+3\lambda^n \tag{244}$$

With $a_1 = -73/60$, $a_2 = 77.293/50.400$, $a_3 = -22.5083$, $a_4 = -5.6117$, $a_5 = -0.3363$, $a_6 = -1.216$, $a_7 = 1.647$, $b_1 = 7/60$, $b_2 = -2.227/50.400$, $b_3 = 4.0180$, $b_4 = -3.9788$, $b_5 = -1.9215$, $b_6 = 4.392$ and $b_7 = 5.006$.

For cylindrical geometry pores, θ_i can be written as:

$$\theta_i = \left(1-\lambda_i\right)^2 \tag{245}$$

For a slit-like pore geometry, were used the expressions for $K_{i,c}$ and $K_{i,d}$ as below:

$$K_{i,d} = 1-1.004\lambda_i+0.418\lambda_i^3+0.21\lambda_i^4-0.169\lambda_i^5 \tag{246}$$

$$K_{i,c} = \frac{3-\theta_i^2}{2}\left(1-\frac{\lambda_i^2}{3}\right) \tag{247}$$

where the steric partitioning coefficient was given by (according to its definition):

$$\theta_i = \left(1 - \lambda_i\right) \tag{248}$$

It should be noted that there is several research conduct the assumption of the hindered factors of diffusion and convection $K_{i,c}$, $K_{i,d}$, we took the work of Geraldes and Brites Alves [101] where they introduced new forms of hindered factors of diffusion and convection were given as follows:

$$K_{i,c} = \frac{1 + 3.867\lambda_i - 1.907\lambda_i^2 - 0.834\lambda_i^3}{1 + 1.857\lambda_i - 0.741\lambda_i^2} \tag{249}$$

For the hindered factor of diffusion $K_{i,d}$, it is related to the functions of the solute radius-pore radius ratio.

If $\lambda_i \leq 0.95$:

$$K_{i,d} = \begin{pmatrix} 1 + \left(\frac{9}{8}\right)\lambda_i \ln\lambda_i - 1.56034\lambda_i + 0.528155\lambda_i^2 + 1.91521\lambda_i^3 - \\ 2.81903\lambda_i^4 + 0.270788\lambda_i^5 - 1.10115\lambda_i^6 - 0.435933\lambda_i^7 \end{pmatrix} / \theta_i \tag{250}$$

If $\lambda_i > 0.95$:

$$K_{i,d} = 0.984\left(\frac{1 - \lambda_i}{\lambda_i}\right)^{5/2} \tag{251}$$

5. Straatsma et al. model (Generalized Maxwell–Stefan model)

Straatsma et al. [102] studied the phenomena of nanofiltration transfer in the way to give a fully predicted model for the case of uncharged solute (glucose), single salt solution (sodium chloride, calcium chloride and sodium sulfate) and ternary ions mixture of those salts; their model based on the Maxwell–Stefan equation.

To describe the transport phenomena in this model four transport layers are distinguished: (1) a stagnant layer where concentration polarization of components that do not fully pass the membrane takes place; (2,3) interface layers at bulk/membrane and membrane/permeate boundary; (4) the membrane layer itself.

The frequent expression of the Maxwell–Stefan relation of solutes *i*, design for one direction (*y*) is:

$$-\frac{d\mu_i}{dy} - \frac{V_{m,i}dP}{dy} - z_i \cdot F\frac{d\varphi}{dy} = \sum_{j=1}^{n} x_j \cdot \zeta_{i,j}\left(v_{d,i} - v_{d,j}\right) \tag{252}$$

It is well known that the concentrations in the pore of the membrane differ from the concentration in the liquid because of the steric and electrostatic exclusion. The interface layer in which the concentration changes take place is very thin, so we can neglect the friction losses.

In the interface layer (Eq. (252)) would be written as:

$$\Delta\mu_0 + V_i \cdot \Delta P_0 + z_i \cdot F \cdot \Delta\varphi_0 = 0 \tag{253}$$

The expression of chemical potential difference ($\Delta\mu$) can be given as:

$$\Delta\mu_0 = R_g T \ln\left(\frac{\gamma_{0,i}}{\theta_i \cdot \gamma_i}\right) \tag{254}$$

where θ_i is the steric factor, which depends on both radius (solute (r_s) and pore (r_p)) based on the Ferry expression as presented in Eq. (106).

For transport through a membrane some extensions were needed in the application of the common Maxwell–Stefan equation; as a first step Straatsma et al. [102] added a friction force of solute *i* with a membrane F_m as illustrated in Eq. (255). Besides diffusive transport, viscous flow occurs in pressure-driven membrane processes and the viscous velocity (v_v) written as Eq. (255):

$$F_m = \zeta_{i,M} \cdot v_{d,i} \tag{255}$$

$$v_v = -\frac{A}{u} \cdot \frac{dP}{dy} \tag{256}$$

With *A* was taken as hydraulic permeability.

They replaced v_d with:

$$v_d = v_t - v_v \tag{257}$$

where v_t is denoted to the total velocity. The combination of Eqs. (252) and (255)–(257) results in:

$$-\frac{d\mu_i}{dy} - \frac{V_i + \left(\frac{A}{\mathrm{u}} \cdot \zeta_{i,M}\right)dP}{dy} - z_i \cdot F\frac{d\varphi}{dy} = \sum_{j=1}^{n}\left(x_j \cdot \zeta_{i,J}\left(v_{d,i} - v_{d,j}\right)\right) + \zeta_{i,M} \cdot v_d \tag{258}$$

It should be noted that if the membrane is highly charged so the Eq. (256) is not applicable for highly viscous flow, then were used the assumption in which we consider both flows diffusive and viscous as a whole and we changed the diffusive frictions factors (ζ) that exist in Eqs. (252) and (255) by overall friction coefficients (ξ):

$$-\frac{d\mu_i}{dy} - \frac{V_{m,i}dP}{dy} - z_i \cdot F\frac{d\varphi}{dy} = \sum_{j=1}^{n}\left(x_j \cdot \xi_{i,j}\left(v_i - v_j\right)\right) + \xi_{i,M} \cdot v_i \tag{259}$$

The expression of chemical potential for solute *i* (μ_i) as used in Eqs. (252) and (259) it is written as:

$$\mu_i = RT \cdot \ln\gamma_i \tag{260}$$

where $\gamma_{i,M}$ the molar activity is given as:

$$\gamma_{i,M} = \gamma_i \cdot x_i \tag{261}$$

The friction coefficient between solutes in the absence of any charge effects was estimated as:

$$\zeta_{i,j} = \sqrt{\zeta_{i,w} \cdot \zeta_{j,w}} \tag{262}$$

While $\zeta_{i,w}$ and $\zeta_{j,w}$ are respectively the friction coefficients in the water. In which the friction coefficients between cation and anion was calculated using this empirical expression:

$$\zeta_{\text{anion,cation}} = 8.6 \cdot 10^{-13} \cdot \zeta_{i,w} \cdot \zeta_{j,w} \cdot \frac{\left|z_i \cdot z_j\right|^{1.85}}{I^{0.55}} \tag{263}$$

I represent the ionic strength.

Where they calculated the diffusive friction coefficient between solute-membrane using the expression below:

$$\zeta_{i,M} = \zeta_{i,w} \cdot \left(\left(1 - \frac{r_i}{r_p} \right)^{-2.2} - 1 \right) \tag{264}$$

The viscous friction coefficient (ζ_v) depends on the hydraulic permeability (A) as in this relation:

$$\zeta_V = \frac{\text{u}}{A \cdot C_i} \tag{265}$$

The global friction coefficients between (solutes-solutes ($\xi_{i,j}$) and solute-membrane ($\zeta_{i,M}$))can be derived from the diffusive friction coefficients as well as viscous friction coefficients by neglecting the effect of viscous selectivity; with this assumption, the relation of the mixture systems reduces to:

$$\xi_{\text{anion,cation}} = \xi_{\text{cation,anion}} = \zeta_{\text{anion,cation}} + \zeta_{i,M} \cdot \frac{\zeta_{j,M}}{\zeta_V + \sum_{k=1}^{n} \left(x_k \cdot \zeta_{k,M} \right)} \tag{266}$$

And,

$$\xi_{i,M} = \zeta_{i,M} \cdot \zeta_V / \zeta_V + \sum_{k=1}^{n} \left(x_k \cdot \zeta_{k,M} \right) \tag{267}$$

In their work they used Freundlich isotherm to calculate the membrane charge:

$$Q_m = Q_0 + \left(\sum_i \left| z_i \right| x_i \right)^{g} \tag{268}$$

where Q_0, g and x_i respectively are model constants and the mole-fraction in the pores.

6. Teorell–Meyer–Sievers model

Teorell–Meyer–Sievers [62] discussed the fundamental mechanism of characteristics such as membrane potential, diffusion coefficient, transport number, electric conductivity, etc. based on the membrane phenomenon in an aqueous electrolyte solution. The TMS model was developed based on the Donnan equilibrium theory and the extended Nernst–Planck equation. This model is a rigorous approach that has been widely used to describe the membrane electrical properties (in the case of a negatively charged membrane) by assuming a uniform radial distribution of fixed charges and mobile species.

For 1-1 type of electrolyte (e.g., NaCl), the membrane parameters can be written as follows:

$$\sigma = 1 - \frac{2}{\left(2\alpha^* - 1\right)\xi^* + \left(\xi^{*2} + 4\right)^{\frac{1}{2}}} \tag{269}$$

$$B = D_i \left(1 - \sigma\right) \left(\frac{\varepsilon}{\delta} \right) \tag{270}$$

where α^* represents the transport numbers of the cation in free solution and ξ^* is the electrostatic parameter. Both nomenclatures can be defined by the following expressions:

$$\alpha^* = \frac{D_{\text{cation}}}{D_{\text{cation}} + D_{\text{anion}}} \tag{271}$$

$$\xi^* = \frac{X_M}{c_i} \tag{272}$$

where D_{cation} and D_{anion} are the diffusivities of cation and anion, respectively, and X_M and c_i are the fixed charge density and the solute concentration of feed solution, respectively. However, the fixed charge density of most of the practically charged membranes varies with the solute concentrations, thus the effective fixed charge density X_M^N was proposed by Wang et al. [103] to replace X as follows:

$$X_M^N = A^\circ \cdot \frac{c_i^{1/2}}{1 + B^\circ c_i^{1/2}} \tag{273}$$

where $A°$ and $B°$ are the empirical coefficients obtained from the permeation experiments of a salt.

7. Steric hindrance pore model and Hagen–Poiseuille model

The steric hindrance pore (SHP) [62] model is adopted to give a better description of the separation properties of the membrane with respect to two key parameters, pore radius, r_p and membrane porosity-thickness ratio, ε/δ. Through modifying the pore model, Nakao and Kimura [104] proposed that the SHP model that can be used to calculate r_p and ε/δ in the case of if single neutral solute. Those two parameters can be written as:

$$\sigma = 1 - H_F \cdot S_F \tag{274}$$

$$B = H_D \cdot S_D \cdot D_i \left(\frac{\mu}{\delta} \right) \tag{275}$$

The nomenclature of Eqs. (Z.1) and (Z.2) can be defined as follow: $H_F = 1 - 16/9\lambda^2$, $H_D = 1$, $S_F = (1 - \lambda)^2[2 - (1 - \lambda)^2]$, $S_D = (1 - \lambda)^2$, $\lambda = r_s/r_p$.
where H_D and H_F, are the steric parameters related to the wall correction factors in the convection coefficient and diffusion coefficient, respectively, and S_F and S_D are the distribution

coefficients of solute in the convection condition and diffusion condition, r_s and r_p are the pore radius of solute and membrane, respectively. To determine the solute diffusivity where the solute is diluted in the water, the Wilke–Chang correlation is often used.

$$D_i = 1.173 \cdot \frac{10^{-16}\left(\vartheta_j \cdot M_j\right)^{\frac{1}{2}} T}{\upsilon \cdot V_{\mathrm{iB}}^{0.6}} \tag{276}$$

where V_{iB} is the solute molar volume at boiling point, T is the temperature, ϑ_j, M_j, and υ are an "association parameter," molecular weight, and viscosity of the water, respectively.

Several assumptions are made in this pore model to determine the membrane properties which they:

- Pore-wall effects on solute moving across the pore are neglected.
- There is no discrepancy between the both model SHP and the fiction model.

On the other hand, water flux through uniform cylindrical pores where no significant concentration gradient is present across the membrane can be described by the Hagen–Poiseuille equation as follows:

$$j_i = \varepsilon \cdot r_p^2 \cdot \frac{\Delta P}{8 \cdot \upsilon \cdot \tau \cdot \delta} \tag{277}$$

8. Discussion

In this section, we illustrate each model described above, in the terms of commonly used assumptions, the advantages as well as the shortcomings noticed by the membrane researcher community related to the subject.

In this review we have presented state-of-the-art transport phenomena within nanofiltration membranes according to four basic axes: SDM, IT models, Nernst–Planck equation models (ENP) and the Maxwell–Stefan model.

As we started, the SDM presented by Jonsson [55], Wijmans and Baker [56] and Rautenbach and Groschl [57–59], which was based on the following assumptions:

- The permeants dissolve in the membrane material and then diffuse through the membrane down a concentration gradient.
- Constant material properties and ideal sorption and diffusion behavior.
- There is a uniform pressure gradient along the membrane.
- The chemical potential gradient across the membrane was expressed only as a concentration gradient.
- There is no coupling between the water and the solute fluxes.

The net outcome for application of the SDM model gives a better explication of the separation procedure in non-porous and non-charged membranes, only two parameters needed to be found experimentally and the fundamental equations describing transport in this model can be derived from simple, basic principles without resource to process-specific factors. On the other hand, the main disadvantages of the SDM model depict the limitation of this latter in term of solute flux which in the SDM the rejection is independent of solute concentration and reach the unity at significantly high transmembrane water flux, ignoring the electrostatic effect which plays a dominant role in transfer within nanofiltration membrane.

Consequently, the solution–diffusion model is a phenomenological model. The solute permeability parameter in SDM can be different for membranes, which is affected by electrostatic effects. Although the electrostatic effect is not mentioned in model equations, it's combined in phenomenological parameters, which wasn't the case for the transport via nanofiltration porous membranes which were based on the convection. Yaroshchuk et al. [105] extended the solution–diffusion-film model to the case of electrolyte mixture consisting of a single dominant salt and (any number of trace ions) in which they developed a quasi analytical protocol for concentration polarization, in their study they used the same assumption as the solution–diffusion model which is no convective coupling between the solute and water inside the membrane (the same reflection coefficient for all solutes assumed equal to one) in addition they introduced a virtual solution that could be in thermodynamic equilibrium with a given infinitely small volume inside the membrane. Future work mentioned by Reig et al. [106] in which were determinate the reliability of the data obtained using a flat-sheet (FS) laboratory-scale configuration when nanofiltration membranes are implemented at industrial scale level using spiral-wound (SW) configuration. The solution–diffusion–electromigration–film–model (SDEFM) was used to describe the experimental results, in which this model considers that the solute transport through the membrane occurs via solution–diffusion and electric migration phenomena making the convection term negligible [107], also they take into account the concentration polarization layer.

The net outcomes for application of the SDEFM model are capable to fit satisfactorily experimental data of a dominant salt with a trace mixture, were determinate the rejection curves for each of the ions vs. the transmembrane flux produced in each experiment, the rejection values obtained can be explained with the effect of the spontaneously arising electric fields [106].

Another example which was based on the solution–diffusion model is the homogenous solution model (HSDM) modified to include film theory; Zhao et al. [108] applied this model to predict salt rejection by tight nanofiltration membranes during pilot-scale applications and developed an approach to correlate the solute mass transport coefficient to the salt type.

The IT models starting with Kedem–Katchalsky model [63] as a fundamental equation which was based on the following assumptions:

- The water and the solute fluxes were related by the reaction between the three parameters (solute/water/membrane).
- The pressure and the concentration gradients had a linear variation in the case of low level of water flow rate near thermodynamic equilibrium expressed by a phenomenological constant.

- Phenomenological constant depended on the salt concentration which introducing by the new parameter named σ sigma (reflexion coefficient).

The advantages of the Kedem–Katchalsky model [63] was limited by, the water and the solute transport across the membrane is characterized by water and solute parameters, this model included a linear equation for dilute two-components non-electrolyte system of water and solute. Based on the previous assumptions Schlögl [64] extended the Kedem–Katchalsky model which he derived an integral formula for non-linear equation of both fluxes (solute/water) for mixture dilute system in which they removed the consideration of membrane morphology by assumed that the kinetic parameters σ_i, A_i are constant in which he involved a new parameter to describe the non-linearity between the driving forces and particles fluxes.

Galey and Van Bruggen [65] also extended Kedem–Katchalsky equations for the case of mixture of multi organic ions in their model they proposed that the flux of each solute is affected by other solute and an existing solute-solute interaction is mainly depend on the solute permeability, concentration and molecular size, in addition, they examine the impact of pore size in the flux ratio and the solute interaction.

Those models presented above Kedem–Katchalsky model [63], Schlögl [64] and Galey and Van Bruggen [65] are limited on the following disadvantages: eliminates the description of the membrane transport mechanism; for Kedem–Katchalsky model [63] was sufficient only for case of dilute two components solution; about Schlögl model [64] which was confirmed only in the case of lower concentration differences between the feed/membrane and membrane/permeate phases; in additional those models doesn't take the impact of surface charge (electro-static effect), pore length or tortuosity the case of nanofiltration membranes.

In contrast, the Spiegler–Kedem model [66] based on the improvement of the Kedem–Katchalsky formula in which they derived the differential non-linear equations of both fluxes (solute and water) after they integrated them to represent the non-linearity between the fluxes and the potential forces of gradient, based on the following assumption:

- They consider the approximate constant value of fluxes and model coefficient L'_p, σ, ω'.
- They related the high flow rate with a high concentration gradient.
- The model coefficients are independent of salt concentration.
- The solute rejection expression is derived for (1-1) electrolyte according to the water flux.

The main advantage of this model lies in the simple application, few parameters needed to implement which the coupling of the water and the salt fluxes are taken into account; However is still an alternative to the complex physical models, mostly used in the single solute and binary solute systems with one solute is assumed to be impermeable to the membrane, as well as that the Spiegler–Kedem model doesn't consider the electrostatic exclusion and the concentration dependence of the rejection.

Perry and Linder [68] improved the Spiegler–Kedem model which will be suitable for mixture of salt and organic ions, in their work they supposed that both coefficients (permeability, reflexion coefficient) had constant value and there is no effect of concentration polarization, The net outcome of this model is that could save time and effort for ultra-purification process with good economic effects; despite that this model cannot be applied for a multi-solutes system and restricted to a single solute of known molar mass and charge. In the work presented by Ahmad et al. [69] they extended the Spiegler–Kedem model in which they assume all solute is semi-permeable to the membrane, each solute has a constant value of diffusion and mass transfer coefficient in concentration polarization layer thickness taking into account the solute-solute interaction.

Unfortunately, the limitations of those models based on the Spiegler–Kedem equation are:

In the case of Spiegler–Kedem model [66] wherein they neglected the solute-solute interaction, the solute rejection measure, without considering the concentration polarization effect, tested only for the case of single electrolyte, also for Perry and Linder [68] a complexity was noticed for the multi-solute system, no global salt permeability and reflexion coefficient was related to the variation of the solute concentration in the feed.

About the case of Ahmad et al. [69] which they neglected the charge of solute and the pressure difference along the vertical length of the membrane surface. In Van der Bruggen and Van de casteele [109] used the Spiegler–Kedem model to predict the removal of uncharged solutes with nanofiltration in which they used the effective diameter as a size parameter, the reflection coefficient distribution and the diffusion parameter can be determined for a given membrane with the log-normal model and Stokes–Einstein's law.

The extended Nernst–Planck equation (ENP) accounts for the passage of solutes via the membrane by three transport mechanisms, diffusion, convection and electro-migration. The transport of convection occurs as a result of the nanofiltration porous nature, hence the negative charge of the membrane plays important roles in the diffusive transport, and electro-migration occurs due to the gradient in electrical potential.

According to Nernst–Planck proposed by Schlögl [64] in which he introduced the convective solute transport along with permeating water; Dresner [77] presented a new approach to simplifier the calculation of extended Nernst–Planck equation which required only a small amount of calculation in the case of hyperfiltration of multi-solute solution in which he resembles the Schlögl–Goldman method for the electric field taking into account the supposition of good co-ion exclusion, then he introduced a coupling coefficient β_i in the original form presented by Schlögl; to simplify the discussion, he consider only thermodynamic system in which the mechanical equilibrium is fulfilled in the term of (the component velocity is independent of the position and the pressure gradient is equal to the sum of external forces). The advantage of the application of the Dresner approach that it needed only a small amount of calculation even when several ions are existing.

Tsuru et al. [78,82] Extended Nernst–Planck equation to calculate the rejection of single and mixed electrolyte solution of various valences using a negatively charged membrane taking into account porosity ration ($\varepsilon/\Delta x$), volume flux, mole friction as well as effective membrane charge density X_d, in which they suppose that the anion mobility inside the pore is the same as in the bulk solution as well as the activity coefficient relation in the membrane and the bulk is equal $\gamma_i^M/\gamma_i = 1$, in their work, they found that for a single salts the rejection related to volume flux with the same evolution as the effective charge density, the same remark for mixture electrolyte the rejection was strongly related to the volume flux, mole friction and the ratio of feed concentration to the effective charge density.

An overview contribution related to this subject was conducted by Bowen and his research team in which they give a real understanding of the transfer phenomena within nanofiltration membranes, starting with hybrid model proposed by Bowen and Mukhtar [83] as DSPM based on the extended Nernst–Planck equation which they solved ENP as if the membrane were homogenous and non-porous, hindrance factors of diffusion and convection were included to allow taking the transport of solute through the membrane which they depend on the ratio of ion radius to pore radius, the effective pore radius (r_p), the effective membrane thickness to the porosity ratio ($\Delta x/\varepsilon$) and the effective membrane charge density (X_M) where the modeling parameters. The effective pore radius was calculated using experimental data for single salt rejection, in which they found that NaCl gives a better result, about the effective membrane charge density they presented in term of Freundlich isotherm as a linear expression depends on the bulk salt concentration; the model was successful in predicting the separation performance of a ternary salt system (Na^+: Cl^-: SO_4^{2-}) the negative rejection of Cl^- at low flux was explained in terms of the interplay between diffusion, convection, and electromigration mechanisms.

Future work presented by Bowen and Mohammad [85] introduced a model for separation solute of salt/dye solution this model was based on DSPM with the incorporation of concentration polarization (film model) for a mixture of charge solute in which they optimizing this process in term of process time, membrane structure and electrical propriety,

wherein they starting by membrane characterized in terms of the effective pore radius (r_p), the effective ratio of membrane thickness over porosity ($\Delta x/\varepsilon$), and the volumetric charge density (X_M), were obtained using the rejection data of uncharged solutes and salts in combination with a Donnan–steric pore model. Using those parameters, which they also included a description of the solution concentration polarization for mixtures of charged solutes in their model. They found out that when the removal of salt in the dye-salt solution is considered through the diafiltration, in which the process needs complete retention of dye with low retentions of sodium and chloride ions, a membrane with a pore size smaller than the effective radius of the dye molecule is a good choice. Membranes with low charges were found to be favorable for the process since they resulted in negative rejections for chloride ions. They also ascertained that a low membrane thickness value shortens the processing time.

Bowen and Welfoot [54] they present an accurate model for a major understanding of the nanofiltration transfer phenomena in which they reduced the calculation parameters of uncharged solute to one parameter (r_p) related to the effective pressure difference according to the hydrodynamics demonstration with hindered solute transport through the pore, also they incorporated the pressure effect on chemical potential and pore radius dependent on viscosity, on the other hand for electrolyte solution they reduced to only two parameters (r_p, X_d) by including dielectric exclusion in the expression of energy barrier for ion partitioning inside the pores so that the revaluation of the pore dielectric constant using the data of NaCl rejection at the membrane iso-electric point gives us a better understanding.

The quantification of DE would be hold by experimental studies of other salts over a range of concentrations at uncharged membranes and the potential would have great importance for the overall rejection at the membrane since the variation of water viscosity and dielectric properties with pore radius exist.

In the ensuing paper Bowen et al. present a linearized model [93] to describe transfer phenomena for electrolyte rejection based on following factors pore radius, membrane charge, pore dielectric constant in which they used for reducing the complexity of the previous differential equation systems by eliminating most of the numerical integration; wherein they introduced the changes in dielectric constant of water between the bulk and the membrane pores, this latter will change the emphasis from the effective membrane charge to the effective pore radius. The comparison of the linearized model and the previous ones based on the numerical integration agreed over a wide range of conditions when the valences or the number of the ions increased, the programming efforts also increased; In addition, linearized model could save time required to generate predictions for rejection of mixture solute systems by at least two orders of magnitude.

According to the many advantages gives by the use of DSPM model for predicting the transfer via nanofiltration membranes several works was based on it, we could cite the following:

Chang et al. [110] presented a comparative performance study of two membranes from the same manufacturer (nanofiltration and low-pressure RO) in the term of As(III) rejection, under a variety of operating conditions, they used a predicted model based on the DSPM for make comparison between the model results and the experimental results, in which they found an over-estimated values of rejection ratio obtained by this model, this over-estimation was explained by the use of larger molecular size arsenite than the real.

Déon et al. [111] implemented a dynamic model with an improvement of the Donnan-Steric-pore model for single salt solution (NaCl, $MgCl_2$, Na_2SO_4) of 10 mol/m^3 for filtration in concentration mode and the feed concentration was set at 100 mol/m^3 for diafiltration which includes both volume and concentration variation over time is proposed, this model was suggested to treat a real effluent in nanofiltration for both cases concentration or diafiltration which the previous models were failing in the case of concentration progressively evolve due to collected of permeate stream. The parameters of the transport model were identified by fitting experimental results at a constant concentration before being used to predict the performance evolution over time, taking into account the variation of the membrane charge due to the evolution of concentration over time through the use of adsorption isotherm.

This model proposed by Déon et al. [111] was successful in predicting the one-time and overall performance of the nanofiltration process during the filtration of various salt solutions in both concentration and diafiltration mode.

Hagmeyer and Gimble [86,87] introduced a model to predict the performances of nanofiltration membranes based on TMS and NP to investigate the rejection of the ternary solute mixtures NaCl–Na_2SO_4 and NaCl–CaCl. They included the energy term in their model and proposed an empirical relation to incorporate the effect of the dielectric constant change between the bulk solution and the solution in the pore along with the membrane dielectric constant to calculate the energy difference term in which they used zeta potential measurement to calculate the membrane surface charge density. The main objective is to reduce the amount of needed fitting parameters in the case of the constant potential of the membrane surface to two membrane parameters, which are independent of the composition of the bulk solution. These are the ratio of pore density to membrane thickness and the pore radius, taking into account the supposition of constant potential.

Afonso and Depinho [90] integrated a model to predict a nanofiltration performance in term of membrane permeability, selectivity as a function of the salt nature and concentration where the transport of mixture through an amphoteric nanofiltration membrane conduct by combining extended Nernst–Planck equation and Donnan equilibrium at the membrane interface in the case of a single solution of $MgSO_4$, $MgCl_2$ and Na_2SO_4 taking into account the mass transfer mechanisms in those layers (the feed solution, the bulk/ membrane, membrane active layer) wherein the concentration polarization is described by correlation derived from tubular turbulent flow and high permeation fluxes.

The membrane effective charge parameter is found to depend on the solute nature and concentration; wherein the relative errors found between the experimental and the calculated permeation fluxes and salt rejections are lower than 22% and 12%.

Lefebvre et al. [94,95,112] used hybrid HETT for predict a nanofiltration transport for a multi-solute mixture (NaCl–$CaCl_2$) from the single salt result wherein was considered hindrance factors in transport and Donnan–steric partitioning; the difference between their model and DSPM model was in the pore radius in which they changed by bare ion crystal radius or (Pauling radius).

Theoretical solute rejection predictions for multi-electrolyte solutions are obtained by numerically solving the hindered transport extended Nernst–Planck (ENP) ions flux equations using the computer simulation program, NANOFLUX, which incorporates electrostatic, steric, and hydrodynamic interactions and a new choice for ion size (bare crystal, or Pauling, radius). Lefebvre et al. [94,95] concluded that their method could lead to a cost-effective way for choosing appropriate nanofiltration membranes, optimizing the implementation of industrial nanofiltration processes, and finally dimensioning industrial-scale nanofiltration plants.

Vezzani and Bandini [96,97] implemented a general model taking into account the difference in the dielectric constant of the solution in the pore and the membrane called DSPM-DE; the determination of the rejection mechanism which is related to dielectric effect was supposed by the role of the difference existing between both dielectric constants (the aqueous solution in the pores and in the membrane material). Several adjustable parameters which characterize the membrane such as (the volumetric charge density, the average pore radius as well as the effective membrane thickness). In this model, ionic partitioning at the interfaces between the membrane and the external phases takes into account three separation mechanisms: steric hindrance, Donnan equilibrium, and dielectric exclusion; in which they don't notice the dielectric effect in case of mixtures containing various co-ions, such as NaCl + Na_2SO_4 [112].

Future work proposed by Roy et al. [113] aims at introducing a comprehensive model by extending the DSPM-DE model for flat-sheet and spiral-wound for large-scale nanofiltration membranes and evaluates their performance for the seawater desalination application.

This model was introduced for analyzing commercially used nanofiltration elements that allow the user to understand the mechanism of filtration and provides the flexibility to simulate a wide range of membrane types by adjusting the various key parameters that characterize the membrane. In their study has shown that the rejection and the recovery ration of the nanofiltration membrane were dependent on the net driving pressure across the membrane in which the net driving pressure increases with feed pressure it increases with an increase in feed flow rate until hydraulic pressure losses become dominant.

Aleman and Dickson [98] predict the performance of nanofiltration membranes by one-dimensional mathematical model based on three fundamentals theory (Extended Nernst–Planck, Donnan equilibrium and Gouy–Chapman theory) wherein they incorporate to the classical DSPM model the Gouy–Chapman equation for the calculation of the membrane charge by assuming that the solute adsorption is purely electrostatic in the case of mixed electrolyte solution in which that this model consists only three fitting parameters (L_p, r_p, φ), two solutions (flat and cylindrical surface) of Gouy–Chapman theory is used and compared.

SEDE developed by Szymczyk and Fievet [99] by using the dielectric al exclusion mechanism into the classical theory (steric/electric exclusion), the main objective is to investigate the transfer phenomena within nanofiltration membranes in which they improved a model to describe this transfer for both geometries (cylindrical and slit-like) pore by using a new mechanism of the dielectric exclusion taking into account both terms (Born effect and image forces).

This model used to measure the membrane rejection rate and dielectric constant of the solution taking into account only the filling pores as adjustable parameter in this model The distribution of solutes at the membrane/solution interfaces is described as being the result of (size effects, Donnan exclusion and dielectric effects) these are expressed as sum of multi-terms: Born dielectric effect (which is related with the diminution of the dielectric constant of a solution inside nanopores), production of image forces increasing due to (the difference in dielectric constants between the membrane matrix and the solution filling pores).

Szymczyk and Fievet has shown that the dielectric exclusion plays a major role in the retention mechanism of the nanofiltration polyamide membrane and that the widely adopted steric/electric exclusion theory is not suitable to describe transport properties of such a membrane.

A future approach have been developed by Silva et al. [114] in which they incorporated the variation of charge inside the membrane pore to the previous model described by Szymczyk and Fievet (Steric-Electric and dielectric exclusion model) wherein were used to model the system, structural, electrical and dielectric al membrane parameters to study the rejection of single and divalent salts and a mixture of them. Multi-solute solutions of $NaCl–Na_2SO_4$ and $NaCl–MgCl_2$ have been used to measure the retention of each one.

The main objective of Silva et al. [114] study is investigating the effect of a common counter-ion and co-ion in nanofiltration for concentrated solutions, regarding the separation performance and electrical behavior.

Silva et al. [114] indicate that the SEDE-VCh model is able to describe the transport phenomena involved in both the studied systems, including both single and multi-solute mixtures, by using only three fitting parameters dielectric constant inside the pore, the effective diameter of solute and the bulk phase for a slit geometry.

Straatsma et al. [102]used generalized Maxwell–Stefan (GMS) transport equations to model the single salts and multi-solute electrolyte solutions with a common as a function of membrane properties (mean pore size, porosity, thickness, surface charge characteristic) and feed pressure. Generalized Maxwell–Stefan (GMS) equation takes into account ion interactions represented in terms of frictions of the solutes with each other. In this work Straatsma et al. [102] taking into account that the Maxwell–Stefan transport relations mentioned both frictions coefficients (diffusive ($\zeta_{i,j}$ and $\zeta_{i,M}$) and overall ($\xi_{i,j}$ and $\zeta_{i,M}$)) appeared, wherein the diffusive interaction between two solutes was related to their type.

Hoshyargar et al. [115] developed a comprehensive mathematical model for the prediction of solutes transport through nanofiltration membrane based on Maxwell–Stefan approach which consider a multi-solute transport in two sections of the membrane system: boundary layer and membrane the main assumptions considered in this model was:

- All solutes have a constant molar flux at the steady-state condition.
- The transport process in the membrane is isothermal.
- The charge density is non-uniform along the pore, unlike many studies, considering probable solute adsorption to the pore wall through the Freundlich isotherm.
- Dielectric exclusion is considered in partitioning when combined with GMS.
- Not assuming linear profile for electric potential and concentration through the membrane.

Taking into account that the interactions of solute/solute, solute/water, water/membrane and solute/membrane in which the model incorporates the membrane microstructural parameters, the solute molecular properties, the feed solution physical properties and the operational conditions into one rigorous mathematical description [115].

The TMS model [116] is a rigorous approach to describe the membrane electrical properties in terms of the effective charge density X_M and electrostatic effects ξ. This model has been extensively used to explain the transport mechanism in nanofiltration membranes considering the electrostatic effects for the permeation of electrolyte (sodium chloride). The TMS model assumes a uniform radial distribution of fixed charges and mobile species, this model can be interpreted using the electrical properties of the membrane [116].

According to the SHP model, the viscosity (υ) is the only water parameter influencing permeation. Although the viscosity equation is usually used for porous membranes, it is also valid for nanofiltration membranes. The Hagen–Poiseuille equation clearly shows the effect of membrane structure on transport as well as the effect of some specific parameters on the membrane performance. It gives a good description of the transport through membranes consisting of circular pores of the same radius, although this is generally not the case in practice [62].

According to the complexity of predicting the transport within nanofiltration membranes, regarding the system interaction, the electrostatic effect, membrane charge, pore geometry, multi-component system, concentration, concentration polarization effect.

The models based on the solution–diffusion which they ignored the electrostatic effect are not possible to use for the case of transport within nanofiltration membrane, unless they incorporate the elector-migration effect as in the case of Reig et al. [106], but still applicable for one dominant solute. About Irreversible Thermodynamic models which originated historically from the modeling of RO processes [53]. In these models, the membrane is treated as a black box. Consequently, the characterization of structural and electrical properties is not possible [54] without considering the interaction between the system (solute/water/membrane) taking into account the effect of the multi-component system; Ahmad et al. [69] give a better contribution to predicting the transport within nanofiltration membranes by extending the Spiegler–Kedem model in the case of multi-component system, but still valid only for the case of binary system.

On the other hand, the extended Nernst–Planck and Maxwell–Stefan models were introduced simultaneously with the advent of nanofiltration to describe the transport of solutes through the membrane via sieving and electrical mechanism [87].

9. Conclusion

This paper has reviewed the main four mathematical models of Solution-Diffusion, irreversible thermodynamics, Extended Nernst–Planck equation and Generalized Stefan–Maxwell equation used for describing the transport phenomena within nanofiltration membranes. The purpose of this comprehensive review is focused on the efficiency of these models under different operating conditions from single salts to mixture system including (solutes valences, concentrations, concentration polarization, solute/solute interaction, solute/water interaction, solute/membrane interaction, electric effect, dielectric effect, Donnan effect, Born effect, image forces...).

Each model provided with a demonstration, theoretical background (governing equations) and discussion in the term of advantage and disadvantage.

Wherein concluded as the basic principle of separation mechanism of the nanofiltration membrane has been identified mostly due to charge and steric effect, according to the models described above:

- The solution–diffusion models that neglected the coupling between the water and the solute fluxes, exclude the concentration and the electrostatic effects wherein it does not fit the principal of nanofiltration membranes.
- The irreversible thermodynamics models was highly dependent on the driving forces which limits their practical application, the system should be adjacent to the equilibrium, limited in the multi-solute systems, in several cases were neglected the solute charge; rather than the solution–diffusion models, this latter had such place on nanofiltration modeling with further improvements.
- A large majority of modeling works on nanofiltration has been by models based on the extended Nernst–Planck equation based on (diffusion, convection and electro-migration) due to the net outcomes given by the latter, which taking into account the interaction between the system(solute, water and membrane), nature and concentration of solute (charged or uncharged), single or multi-ions, membrane charge, Donnan effect, steric effect, energy barrier wherein give a better understanding to the transfer phenomena within nanofiltration membranes due to the ability of the latter to provide information related to properties of both the membrane and the process stream.

The prediction of nanofiltration membranes performances has been an active area of research; it still needs further improvements in the terms of technical models, software simulators and review papers, to get more understanding of this phenomenon.

Acknowledgment

The authors gratefully acknowledge support from Algerian Ministry of Higher Education and Scientific Research, Bouira University for Laboratory of Energy, Water, Environment, PM3E.

Symbols

a	—	Parameters using in Lefebvre et al. model
A	—	Water permeability coefficient, m³/m²tP
A^*	—	Modified water permeability constant, m³/m²tP
A_{ij}, A_{ji}	—	Cross permeability coefficient between solutes *i* and *j*, cm/s²
A_{ii}, A_{jj}	—	Self-permeability coefficient of solute *i* and solute *j*, cm/s
A_{ws}	—	Cross-phenomenological coefficients of water and solute, *m*
A_{ww}	—	Straight phenomenological coefficients of water
$A°$	—	Empirical coefficients obtained from the permeation experiments of a salt
a_i	—	Activity of ion, mol/m³
b_i	—	Parameters using in Lefbreve et al. model
B	—	Solute permeability constant, mol/m²t
B_{ss}, B_{si}	—	Straight phenomenological coefficients of the solute and solute with ion *i*
B_{sw}	—	Cross-phenomenological coefficients of solute and water, m
$B°$	—	Empirical coefficients obtained from the permeation experiments of a salt
B^*	—	Modified solute permeability constant, mol/m²t
b	—	Solute-membrane friction parameter, dimensionless
b_0	—	Sorption coefficient, m³/mol
b_1	—	Langmuir adsorption coefficient, m³/mol
c_i	—	Concentration of ion *i* in membrane, mol/cm³
C_i, C_{if}	—	Concentration of solute *i* in the feed, mol/cm³
C_p	—	Permeat concentration, mol/cm³
C_w	—	Molar concentration of water, kg/m³ or mol/cm³
C_{sp}	—	Molar concentration of solute at permeat interface, kg/m³ or mol/cm³
C_{pc}	—	Cumulative permeate concentration for a batch process, mol/cm³
C_s^{ave}	—	Represent an average concentration of solute, mol/cm³
C_{sm}	—	Molar concentration of solute at membrane/feed interface, kg/m³ or mol/cm³
C_{tm}	—	Total concentration of water and solute in the membrane, mol/cm³
C_{wl}	—	Wall concentration of ion *i* or uncharged solute, kg/m³ or mol/cm³
C_{wm}	—	Molar concentration of water at membrane interface, kg/m³ or mol/cm³
C_{sf}	—	Molar concentration of water at feed interface, kg/m³ or mol/cm³
C_{sp}	—	Molar concentration of water at permeates interface, kg/m³ or mol/cm³
$C_{\mathrm{dye},f}$	—	Molar concentration of dye in feed solution, kg/m³ or mol/cm³
C_{smf}	—	Solute concentration at feed or bulk side membrane surface, mol/cm³
C_{smp}	—	Solute concentration at permeat side membrane surface, mol/cm³
$C_{\mathrm{anion},1}$, $C_{\mathrm{cation},1}$	—	Concentration of the anion and the cation respectively in the iterface membrane/feed, mol/cm³
$C_{\mathrm{anion},2}$, $C_{\mathrm{cation},2}$	—	Concentration of the anion and the cation respectively in the iterface membrane/permeat, mol/cm³
C'_i, C'_j	—	Mean concentration of the solutes *i* and *j* respectively, mol/cm³
C_X^-	—	Organic ion concentration in the solution, mol/cm³
C'_s	—	Salt concentration in the feed, mol/cm³

d — Thickness of the oriented solvent layer, m
D_s — Diffusion coefficient of the salt in the membrane, cm^2/s
D_i — Diffusion coefficient of ion *i* in water, cm^2/s
D_{ip} — Diffusion coefficient of ion *i* in the pore, cm^2/s
D_{ib} — Diffusion coefficient of ion *i* in the bulk, cm^2/s
D_p — Diffusion coefficient of uncharged solute in the pore, cm^2/s
D_w — Diffusion coefficient of water in the membrane, cm^2/s
D_e — Normalized solute diffusivity, D_{sm}/δ^2, 1/t
D_p^* — Corrected uncharged solute pore diffusion coefficient, m^2 s^{-1}
e — Electronic charge, C
E — Potential field, V
F_m — Molar friction force, N/mol
F_s, F, F_w — Driving forces exerted by solutes *s* and *i* and water
g — Model constant Freundlich equation
h — Parameter defined Bandini and Vanzini model
H_F, H_D — Steric parameters related to the wall correction factors in both convection and diffusion coefficients
I — Ionic strength (salt, total), m
I_M — Ionic strength (salt, total) at the feed/membrane interface, feed side m, m
I_B — Ionic strength (salt, total) in feed/membrane interface, membrane side, m
J_i — Flux, mol/cm^2 s
j_p — Total flux of the membrane, mol/cm^2 s
J_s — Solute flux through the membrane, mol/cm^2 s
$J_{\text{si}}, J_{\text{sj}}$ — Solute flux through the membrane for ion *i* and respectively, mol/cm^2 s
J_w — Total water volume flux, cm/s or mol/cm^2 s
k — Mass-transfer coefficient, m/s
k_b — Boltzmann constant, J/K
K_s, K_m — Distribution coefficients of solute and water between the total membrane phase and the bulk solution
K_i, K_j — Partition coefficient of the solutes *i* and *j* respectively ($K_i = x_{i2}/x_i$), dimensionless
K_{ic} — Hindrance factor for convection
K_{id} — Hindrance factor for diffusion
K_c — Uncharged solute hindrance factor for convection, dimensionless
K_{2eff} — Effective convective coefficient
$\overline{K}$ — Parameter defined in dimensionless
L_i — Coefficient relates the chemical potential with the flux equation
M_j — Molecular weight of ion *j*
m — Flow parameter or feed flow rate for single solute system, cm^3/s
N_i — Mechanical permeability of the pores, m/s atm
N_a — Avorgadro constant, 1/mol
O_i — Interaction parameter mentioned in Ahmad et al. model, m/s mol
P — Pressure, bar or kPa
P_i — Pressure of ion *i*, bar or kPa
P_i — Reference pressure of the ion *i*, bar or kPa

Pe — Péclet number
Pe′ — Modified Péclet number, dimensionless
q_m — Solute adsorption in membrane, mol/L^3
q_{tm} — Total solute adsorption in membrane, mol
q_0 — Henry's law adsorption coefficient, mol adsorbed/mol
q_1 — Langmuir adsorption coefficient, mol/L^3
Q_0 — Model constant Freundlich equation, mol/m^3
Q_m — Membrane charge concentration based on pore volume, mol/m^3
r — Radius of stirrer, m
r_p — Membrane pore radius, m
r_s — Stoke's radius of solute, m
r_B — Bjerrum radius, m
R_g — Universal gas constant, 8.31 Pa m^3/K mol or 0.082 atm m^3/kmol °K
R — Solute retention
Re — Reynolds number
Re$_p$ — Reynolds number in the permeat
S — Membrane surface area, m^2
S_F, S_D — Distribution coefficients of solute in the convection and diffusion
Sh — Sherwood number
Sc — Schmidt number
T — Absolute temperature, K
T_i — Passage, or transmission (ion *i*) (–) or, %
t_c — Time during concentration phase, s
t_d — Time during diafiltration phase, s
u_E — Electrophoretic mobility, V cm^{-1}
$\tilde{u}_i$ — Ion electrochemical potential of component *i*
$\tilde{u}_i^m, \tilde{u}_i^b$ — Ion electrochemical potential of component *I* in the membrane/solution interface and in the bulk solution
v — Solvent velocity in pore, m/s
v_M — Solution velocity across the membrane, m/s
v_p — Permeate solution velocity, m/s
V, V_j — Partial molar volumes of ions *i* and *j* respectively, cm^3/mole
V_s, V_w — Partial molar volumes of solute and of water respectively, cm^3/mole
V_c — Concentrate volume, m^3
V_f — Feed volume, m^3
V_p — Permeat volume, m^3
V_F — Feed volume during diafiltration, m^3
V_{iB} — Solute molar volume at boiling point
w — Stirring speed, s^{-1}
x — Length coordinate or space coordinates in the transport direction, cm
x — Dimensionless membrane depth, z/δ
x_i — Mole fraction of ion *i*
X_j, X_i — Mole fraction of ion *j* and *i* respectively
X_j^+ — Parameter defined in Schlögl model
X_M — Fixed membrane charge density
X_M^N — Effective fixed charge density
y — Uncharged solute function, dimensionless
Y_i — Dimensionless group of ion *i*, dimensionless
Y_p — Permeat water recovery dimensionless
y^d — Dimensionless surface electrical potential
Z — Membrane depth, L
z_i, z_j — Charge of valency of ions *i* and *j*, respectively

Greek

α	—	Parameter defined in Eq. (H.2)
α^*	—	Represent the transport numbers of cation in free solution
β	—	Parameters using in Lefebvre et al. model
β_i	—	Convective coupling coefficient
ΔP	—	Difference of pressure, bar or kPa
ΔC	—	Solute concentration difference, mol/L^3
$\Delta\varphi$	—	Potential difference, V
$\Delta\varphi_\Delta$	—	Donnan potential difference, V
$\Delta\pi$	—	Osmotic pressure difference, bar or Pa
ΔU	—	Streaming potential difference, V
ΔW_i	—	Born solvation energy barrier, J
$\partial q_m/\partial_t$	—	Adsorption rate
λ	—	Ratio of ionic or solute radius to pore radius, friction factor
σ	—	Reflection coefficient
σ_c	—	Surface charge, C/m^2
δ	—	Membrane thickness, m
γ	—	Number of charged groups from the organic ion
γ_i, γ_j	—	Activity coefficient for the ions *i* and *j* respectively, mol/m^3
γ_{iM}	—	Molar activity for the ions *i*, mol/m^3
γ_{ib}, γ_{jb}	—	Activity coefficient for the ions *i* and *j* respectively in the bulk, mol/m^3
γ_{im}, γ_{jm}	—	Activity coefficient for the ions *i* and *j* respectively in the membrane, mol/m^3
$\gamma_{\text{anion},1}$, $\gamma_{\text{cation},1}$	—	Activity coefficient for the anion and the cation respectively in the interface membrane/feed, mol/m^3
$\gamma_{\text{anion},2}$, $\gamma_{\text{cation},2}$	—	Activity coefficient for the anion and the cation respectively in the interface membrane/permeat, mol/m^3
ϕ	—	Potential, V
ϕ_b	—	Potential in the bulk, V
ϕ_m	—	Potential in the membrane, V
ϕ_D	—	Donnan potential, V
∇	—	Debye length, m
∇_{DB}	—	Debye length at the feed/membrane interface, feed side, m
∇_{DM}	—	Debye length at the feed/membrane interface, membrane side, m
ζ	—	Zeta potential, V
ε	—	Porosity
ε_b	—	Dielectric constant of the bulk
ε_p	—	Dielectric constant in the pore
ε_m	—	Dielectric constant of the membrane
ε^0	—	Permittivity of free space, 8.8542×10^{12}C^2/J m
ε^*	—	Dielectric constant of oriented water layer, dimensionless
θ_i	—	Steric partition coefficient of ion *i*
ρ	—	Solution density, kg/m^3
υ	—	Viscosity of solution, Pa s
υ_k	—	Kinematic viscosity, m^2 s^{-1}
ϑ_{Anion}	—	Moles of anions per mole of dissociated salt, mol/mol
$\vartheta_{\text{Cation}}$	—	Moles of cations per mole of dissociated salt, mol/mol
ϑ_j	—	Moles of ions *j* per mole of dissociated salt, mol/mol
η	—	Solvent viscosity in pores, Pa s
η_0	—	Bulk viscosity, Pa s
ζ_v	—	Viscous friction coefficient
ζ	—	Diffusive friction coefficient, kg/s mol
ξ^*	—	The electrostatic parameter
$\widehat{\xi}_f$	—	Normalized membrane charge density, $\widehat{\xi_f} = X_m/c_f$
τ	—	Tortuosity
U+00		
$\varnothing$	—	Surface electrical potential, $J/C = V$
$\in_{i,+}\in_{i,-}$	—	Stoichiometric coefficient for cation and anion

Superscripts

p	—	Pore, permeate
m	—	Membrane
w	—	Water
s	—	Solute
B	—	Bulk
i, *j*	—	Ions
dye,*f*	—	Dye in feed solution

References

[1] R.J. Petersen, Composite reverse osmosis and nanofiltration membranes, J. Membr. Sci., 83 (1993) 81–150.

[2] R. Rautenbach, A. Gröschl, Separation potential of nanofiltration membranes, Desalination, 77 (1990) 73–84.

[3] J. Kucera, Reverse Osmosis: Design, Process and Application for Engineers, 2nd ed., Wiley Scrivener Publishing, Beverly, 2015.

[4] Y. Han, Z. Xu, C. Gao, Ultrathin graphene nanofiltration membrane for water purification, Adv. Funct. Mater., 23 (2013) 3693–3700.

[5] H.C. Van der Horst, J.M.K. Timmer, R.J. Leeders, Use of nanofiltration for concentration and demineralization in the dairy industry: model for mass transport, J. Membr. Sci., 104 (1995) 205–218.

[6] D. Peshev, L.G. Peeva, G. Peev, I.I.R. Baptista, A.T. Boam, Application of organic solvent nanofiltration for concentration of antioxidant extracts of rosemary (*Rosmarinus officiallis* L.), Chem. Eng. Res. Des., 89 (2011) 318–327.

[7] A.M. Mika, R.F. Childs, J.M. Dickson, Ultra-low pressure water softening: a new approach to membrane construction, Desalination, 121 (1999) 149–158.

[8] H.S. Alkhatim, M.I. Alcaina, E. Soriano, M.I. Iborra, J. Lora, J. Arnal, Treatment of whey effluents from dairy industries by nanofiltration membranes, Desalination, 119 (1998) 177–183.

[9] A. Román, J. Wang, J. Csanádi, C. Hodúr, G. Vatai, Partial demineralization and concentration of acid whey by nanofiltration combined with diafiltration, Desalination, 241 (2009) 288–295.

[10] E. Vellenga, G. Tragardh, Nanofiltration of combined salt and sugar solutions: coupling between retentions, Desalination, 120 (1998) 211–220.

[11] H.J. Zwijnenberg, A.M. Krosse, K. Ebert, K.V. Peinemann, F.P. Cuperus, Acetone-stable nanofiltration membranes in deacidifying vegetable oil, J. Am. Oil Chem. Soc., 76 (1999) 83–87.

[12] S. Cartier, M.A. Theoleyre, M. Decloux, Treatment of sugar decolorizing resin regeneration waste using nanofiltration, Desalination, 113 (1997) 7–17.

[13] S. Wadley, C.J. Brouckaert, L.A.D. Baddock, C.A. Buckley, Modeling of nanofiltration applied to the recovery of salt from waste brine at a sugar decolorization plant, J. Membr. Sci., 102 (1995) 163–175.

[14] A. Srivastava, A.N. Pathak, Modern technologies for distillery effluent treatment, J. Sci. Ind. Res., 57 (1998) 388–392.

[15] J.M.K. Timmer, H.C. van der Horst, T. Robbertsen, Transport of lactic acid through reverse osmosis and nanofiltration membranes, J. Membr. Sci., 85 (1993) 205–216.

[16] J.M.K. Timmer, J. Kromkamp, T. Robbertsen, Lactic acid separation from fermentation broths by reverse osmosis and nanofiltration, J. Membr. Sci., 92 (1994) 185–197.

[17] I.S. Han, M. Cheryan, Nanofiltration of model acetate solutions, J. Membr. Sci., 107 (1995) 107–113.

[18] J.M.K. Timmer, M.P.J. Speelmans, H.C. van der Horst, Separation of amino acids by nanofiltration and ultrafiltration membranes, Sep. Purif. Technol., 14 (1998) 133–144.

[19] J. Sojka Ledakowicz, T. Koprowski, W. Machnowski, H.H. Knudsen, Membrane filtration of textile dyehouse wastewater for technological water reuse, Desalination, 119 (1998) 1–10.

[20] R.W. Bowen, W.A. Mohammad, A theoretical basis for specifying nanofiltration membranes - dye/salt/water streams, Desalination, 117 (1998) 257–264.

[21] J. Wu, M. Eiteman, S.E. Law, Evaluation of membrane filtration and ozonation processes for treatment of reactive-dye wastewater, J. Environ. Eng., 124 (1998) 272–277.

[22] A. Cassano, E. Drioli, R. Molinari, Recovery and reuse of chemicals in unhairing, degreasing and chromium tanning processes by membranes, Desalination, 113 (1997) 251–261.

[23] A. Cassano, E. Drioli, R. Molinari, C. Bertolutti, Quality improvement of recycled chromium in the tanning operation by membrane processes, Desalination, 108 (1997) 193–203.

[24] K.H. Ahn, H.Y. Cha, I.T. Yeom, K.G. Song, Application of nanofiltration for recycling of paper regeneration wastewater and characterization of filtration resistance, Desalination, 119 (1998) 169–176.

[25] M. Manttari, J.N. Jokinen, M. Nystrom, Influence of filtration conditions on the performance of NF membranes in the filtration of paper mill total effluent, J. Membr. Sci., 137 (1997) 187–199.

[26] M.D. Afonso, M. Norberta De Pinho, Nanofiltration of bleaching pulp and paper effluents in tubular polymeric membranes, Sep. Sci. Technol., 32 (1997) 2641–2658.

[27] M.D. Afonso, M. Norberta De Pinho, Treatment of Bleaching Effluents by Pressure-Driven Membrane Processes - A Review, A. Caetano, M. Norberta de Pinho, Drioli, H. Muntau, Eds., Membrane Technology: Applications to Industrial Wastewater Treatment, Kluwer Academic Publishers, The Netherlands, 1995, pp. 63–79.

[28] V. Geraldes, M. Norberta de Pinho, Process water recovery from pulp bleaching effluents by an NF/ED hybrid process, J. Membr. Sci., 102 (1995) 209–221.

[29] M.J. Rosa, M. Norberta de Pinho, The role of ultrafiltration and nanofiltration on the minimisation of the environmental impact of bleached pulp effluents, J. Membr. Sci., 102 (1995) 155–161.

[30] M.B. Hagg, Membranes in chemical processing. A review of applications and novel developments, Sep. Purif. Methods, 27 (1998) 151–168.

[31] K.F. Lin, Bromide Separation and Concentration using Semi-Permeable Membranes, U.S. Patent, 19 (1995) 5458781.

[32] L.P. Raman, M. Cheryan, N. Rajagopalan, Consider nanofiltration for membrane separations, Chem. Eng. Prog., 90 (1994) 68–74.

[33] C. Jönsson, A.S. Jönsson, The influence of degreasing agents used at car washes on the performance of ultrafiltration membranes, Desalination, 100 (1995) 115–123.

[34] C. Visvanathan, B.D. Marsono, B. Basu, Removal of THMP by nanofiltration: effects of interference parameters, Water Res., 32 (1998) 3527–3538.

[35] J. Schaep, B. Van der Bruggen, S. Uytterhoeven, R. Croux, C. Van de casteele, D. Wilms, E. Van Houtte, F. Vanlerberghe, Removal of hardness from groundwater by nanofiltration, Desalination, 119 (1998) 295–302.

[36] E. Wittmann, P. Cote, C. Medici, J. Leech, A.G. Turner, Treatment of a hard borehole water containing low levels of pesticide by nanofiltration, Desalination, 119 (1998) 347–352.

[37] N.A. Braghetta, F. DiGiano, W.P. Ball, NOM accumulation at NF membrane surface: impact of chemistry and shear, J. Environ. Eng., 124 (1998) 1087–1098.

[38] A.I. Schafer, A.G. Fane, T.D. Waite, Nanofiltration of natural organic matter: removal, fouling and the influence of multivalent ions, Desalination, 118 (1998) 109–122.

[39] M. Alborzfar, G. Jonsson, C. Gron, Removal of natural organic matter from two types of humic ground waters by nanofiltration, Water Res., 32 (1998) 2983–2994.

[40] B. Van der Bruggen, J. Schaep, W. Maes, D. Wilms, C. Vandecasteele, Nanofiltration as a treatment method for the removal of pesticides from ground waters, Desalination, 117 (1998) 139–147.

[41] P. Brandhuber, G. Amy, Alternative methods for membrane filtration of arsenic from drinking water, Desalination, 117 (1998) 1–10.

[42] T. Urase, J.I. Ohb, K. Yamamoto, Effect of pH on rejection of different species of arsenic by nanofiltration, Desalination, 117 (1998) 11–18.

[43] B. Lew, L. Trachtengertz, S. Ratsin, G. Oron, A. Bick, Brackish groundwater membrane system design for sustainable irrigation: optimal configuration selection using analytic hierarchy process and multi-dimension scaling, Front. Environ. Sci., 2 (2014) 56 1–10.

[44] A.H. Mahvi, M. Malakootian, A. Fatehizadeh, M.H. Ehrampoush, Nitrate removal from aqueous solutions by nanofiltration, Desal. Wat. Treat., 29 (2011) 326–330.

[45] J. Shen, A. Schäfer, Removal of fluoride and uranium by nanofiltration and reverse osmosis: a review, Chemosphere, 117 (2014) 679–691.

[46] L. Meihong, Y. Sanchuan, Z. Yong, G. Congjie, Study on the thin-film composite nanofiltration membrane for the removal of sulfate from concentrated salt aqueous: preparation and performance, J. Membr. Sci., 310 (2008) 289–295.

[47] C. Blöcher, C. Niewersch, T. Melin, Phosphorus recovery from sewage sludge with a hybrid process of low pressure wet oxidation and nanofiltration, Water Res., 46 (2012) 2009–2019.

[48] J.A. Westrick, D.C. Szlag, B.J. Southwell, J. Sinclair, A review of cyanobacteria and cyanotoxins removal/inactivation in drinking water treatment, Anal. Bioanal. Chem., 397 (2010) 1705–1714.

[49] A.A. Abbas, G. Jingsong, L. Zhi Ping, P. Ying Ya, W.S. Al-Rekabi, Review on landfill leachate treatments, Am. J. Appl. Sci., 6 (2009) 672–684.

[50] Y.K. Kharaka, G. Ambats, T. Presser, R.A. Davis, Removal of selenium from contaminated agricultural drainage water by nanofiltration membranes, Appl. Geochem., 11 (1996) 797–802.

[51] J. Wagner, Membrane Filtration Handbook: Practical Tips and Hints, 2nd ed., Osmonics Inc., USA, 2001.

[52] B. Shi, P. Marchetti, D. Peshev, S. Zhang, A.G. Livingston, Performance of spiral-wound membrane modules in organic solvent nanofiltration–fluid dynamics and mass transfer characteristics, J. Membr. Sci., 494 (2015) 8–24.

[53] C. Bellona, J.E. Drewes, P. Xu, G. Amy, Factors affecting the rejection of organic solutes during NF/RO treatment—a literature review, Water Res., 38 (2004) 2795–2809.

[54] W.R. Bowen, J.S. Welfoot, Modelling the performance of membrane nanofiltration-critical assessment and model development, Chem. Eng. Sci., 57 (2002) 1121–1137.

[55] G. Jonsson, Overview of theories for water and solutes transport in 9 UF/RO membranes, Desalination, 35 (1980) 21–38.

[56] J.G. Wijmans, R.W. Baker, The solution–diffusion model: a review, J. Membr. Sci., 107 (1995) 1–21.

[57] R. Rautenbach, A. Groschl, Reverse Osmosis of Aqueous Organic Solutions: Material Transport and Process Design, Presented at the 1990 International Congress on Membranes and Membrane Processes, Chicago, IL, Aug 20–24, 1990.

[58] R. Rautenbach, A. Groschl, Fractionation of Aqueous Organic Mixtures by Reverse Osmosis, Presented at the 203rd American Chemical Society National Meeting, San Francisco, CA, April 5–10, 1992.

[59] R. Rautenbach, A. Groschl, Fractionation of aqueous organic mixtures by reverse osmosis, Desalination, 90 (1993) 93–106.

[60] M.E. Williams, J.A. Hestekin, C.N. Smothers, D. Bhattacharyya, Separation of organic pollutants by reverse osmosis and nanofiltration membranes: mathematical models and experimental verification, Ind. Eng. Chem. Res., 38 (1999) 3683–3695.

[61] S. Sourirajan, T. Matsuura, Reverse Osmosis/Ultrafiltration Process Principles, National Research Council of Canada, Ottawa, Canada, 1985.

[62] L.W. Jye, A.F. Ismail, Nanofiltration Membranes: Synthesis, Characterization and Application, CRC Press, Taylor & Francis Group, 2017.

[63] O. Kedem, A. Katchalsky, Thermodynamic analysis of the permeability of biological membranes to non-electrolytes, Biochim. Biophys. Acta, 27 (1958) 229–246.

[64] R. Schlögl, Non-linear transport behaviour in very thin membranes, Q. Rev. Biophys., 2 (1969) 305–313.

[65] W.R. Galey, J.T. Van Bruggen, The coupling of solute fluxes in membranes, J. Gen. Physiol., 55 (1970) 220–242.

[66] K.S. Spiegler, O. Kedem, Thermodynamics of hyperfiltration (reverse osmosis): criteria for efficient membranes, Desalination, 1 (1966) 311–326.

[67] P. Schirg, F. Widmer, Characterization of nanofiltration membranes for the separation of aqueous dye-salt solutions, Desalination, 89 (1992) 89–107.

[68] M. Perry, C. Linder, Intermediate reverse osmosis ultrafiltration (RO UF) membranes for concentration and desalting of low molecular weight organic solutes, Desalination, 71 (1989) 233–245.

[69] A.L. Ahmad, M.F. Chong, S. Bhatia, Mathematical modelling and simulation of the multiple solutes system for nanofiltration process, J. Membr. Sci., 253 (2005) 103–115.

[70] D. Van Gauwbergen, J. Baeyens, C. Creemers, Modelling osmotic pressures for aqueous solutions for 2-1 and 2-2 electrolytes, Desalination, 109 (1997) 57–65.

[71] A.L. Ahmad, M.F. Chong, S. Bhatia, Mathematical modelling of multiple solutes system for reverse osmosis process in palm oil mill effluent (POME) treatment, Chem. Eng. J., 132 (2007) 183–193.

[72] S. Wadley, C.J. Brouckaert, L.A.D. Badock, C.A. Buckley, Modelling of nanofiltration applied to the recovery of salt from waste brine at a sugar decolourisation plant, J. Membr. Sci., 102 (1995) 163–175.

[73] V.K. Gupta, S.T. Hwang, W.B. Krantz, A.R. Greenberg, Characterization of nanofiltration and reverse osmosis membrane performance for aqueous salt solutions using irreversible thermodynamics, Desalination, 208 (2007) 1–18.

[74] W. Nernst, Die elektromotorische wirksamkeit der Jonen, Z. Phys. Chem., 4 (1889) 129–181.

[75] M. Planck, Uber die Erregung von Elektrizitat und Warme in Elektrolyten, Annalen der Physik und Chemie H., Band XL, 1890, pp. 561–567.

[76] R. Schlögl, Stofftransport durch Membranen, Darmstadt, Steinkopff-verlag, 1964.

[77] L. Dresner, Some remarks on the integration of the extended Nernst–Planck equations in the hyperfiltration of multicomponent solutions, Desalination, 10 (1972) 27–46.

[78] T. Tsuru, M. Urairi, S. Nakao, S. Kimura, Reverse osmosis of single and mixed electrolytes with charged membranes: experiment and analysis, J. Chem. Eng. Jpn., 24 (1991) 518–524.

[79] J.M.M. Peeters, J.P. Boom, M.H.V. Mulder, H. Strathmann, Retention measurments of nanofiltration membranes with electrolyte solutions, J. Membr. Sci., 145 (1998) 199–209.

[80] J.M.M. Peeters, M.H.V. Mulder, H. Strathmann, Streaming potential measurements as a characterization method for nanofiltration membranes, Colloids Surf., 150 (1999) 247–259.

[81] Y.U. Kobatake, N. Kamo, Transport processes in charged membranes, Prog. Polym. Sci. Jpn., 5 (1973) 257–301.

[82] T. Tsuru, M. Urairi, S. Nakao, S. Kimura, Calculation of ion rejection by extended Nernst–Planck equation with charged reverse osmosis membranes for single and mixed electrolyte solutions, J. Chem. Eng. Jpn., 24 (1991) 511–517.

[83] W.R. Bowen, H. Mukhtar, Characterization and prediction of separation performance of nanofiltration membranes, J. Membr. Sci., 112 (1996) 263–274.

[84] J.D. Ferry, Statistical evaluation of sieve constants in ultrafiltration, J. Gen. Physiol., 20 (1936) 95–104.

[85] W.R. Bowen, A.W. Mohammad, Diafiltration by nanofiltration: prediction and optimization, AIChE J., 44 (1998) 1799–1810.

[86] G. Hagmeyer, R. Gimbel, Modelling the salt rejection of nanofiltration membranes using zeta potential measurements, Sep. Purif. Technol., 15 (1999) 19–30.

[87] G. Hagmeyer, R. Gimbel, Modelling the salt rejection of nanofiltration membranes for ternary ion mixtures and for single salts at different pH values, Desalination, 117 (1998) 247–256.

[88] Hunter, Zeta Potential in Colloid Science Academic, New York, 69, 1981.

[89] M. Born, Volumen and hydratationswärme der ionen, Z. Phys. Chem., 1 (1920) 45–48.

[90] M.D. Afonso, M.N. de Pinho, Transport of $MgSO_4$, $MgCl_2$ and Na_2SO_4 across anamphoteric nanofiltration membrane, J. Membr. Sci., 179 (2000) 137–154.

[91] P. Debye, E. Hückel, The theory of electrolytes I. The lowering of the freezing point and related occurrences, Zeit. für Phys., 24 (1923) 185.

[92] J.N. Israelachvili, Measurement of the viscosity of liquids in very thin films, J. Colloid Interface Sci., 110 (1986) 263–271.

[93] W.R. Bowen, J.S. Welfoot, P.M. Williams, Linearized transport model for nanofiltration: development and assessment, AIChE J., 48 (2002) 760–773.

[94] X. Lefebvre, J. Palmeri, J. Sandeaux, R. Sandeaux, P. David, B. Maleyre, C. Guizard, P. Amblard, J.F. Diaz, B. Lamaze, Nanofiltration modelling: a comparative study of the salt filtration performance of a charged ceramic membrane and an organic nanofilter using the computer simulation program NANOFLUX, Sep. Purif. Technol., 32 (2003) 117–126.

[95] X. Lefebvre, J. Palmeri, P. David, Nanofiltration theory: an analytic approach for single salts, J. Phys. Chem. B., 108 (2004) 16811–16824.

[96] S. Bandini, D. Vezzani, Nanofiltration modelling: the role of dielectric exclusion in membrane characterization, Chem. Eng. Sci., 58 (2003) 3303–3326.

[97] D. Vezzani, S. Bandini, Donnan equilibrium and dielectric exclusion for characterization of nanofiltration membranes, Desalination, 149 (2002) 477–483.

[98] J.G. Aleman, J.M. Dickson, Mathematical modelling of nanofiltration membranes with mixed electrolyte solutions, J. Membr. Sci., 235 (2004) 1–13.

[99] A. Szymczyk, P. Fievet, Investigating transport properties of nanofiltration membranes by means of a steric, electric and dielectric exclusion model, J. Membr. Sci., 252 (2005) 77–88.

[100] A.E. Yaroshchuk, Dielectric of ions from membranes, Adv. Colloid Interface Sci., 85 (2000) 193–230.

[101] V. Geraldes, A.M. Brites Alves, Computer program for simulation of mass transport in nanofiltration membranes, J. Membr. Sci., 321 (2008) 172–182.

[102] J. Straatsma, G. Bargeman, H.C. van der Horst, J.A. Wesselingh, Can nanofiltration be fully predicted by a model?, J. Membr. Sci., 198 (2002) 273–284.

[103] X.L. Wang, T. Tsuru, M. Togoh, S. Nakao, S. Kimura, Evaluation of pore structure and electrical properties of nanofiltration membranes, J. Chem. Eng. Jpn., 28 (1995) 186–192.

[104] S.I. Nakao, S. Kimura, Models of membrane transport phenomena and their applications for ultrafiltration data, J. Chem. Eng. Jpn., 15 (1982) 200–205.

[105] A. Yaroshchuk, X.M. Lladó, L. Llenas, M. Rovira, J. de Pablo, Solution-diffusion-film model for the description of pressure-driven trans-membrane transfer of electrolyte mixtures: one dominant salt and trace ions, J. Membr. Sci., 368 (2011) 192–201.

[106] M. Reig, N. Pagés, E. Licon, C. Valderrama, O. Gibert, A. Yaroshchuk, J.S. Cortina, Evolution of electrolyte mixtures rejection behavior using nanofiltration membranes under spiral wound and flat-sheet configurations, Desal. Wat. Treat., 52 (2014) 1–11.

[107] A. Yaroshchuk, M.L. Bruening, E. Zholkovskiy, Modelling nanofiltration of electrolyte solutions, Adv. Colloid Interface Sci., 268 (2019) 39–63.

[108] Y. Zhao, J. Taylor, S. Hong, Combined influence of membrane surface properties and feed water qualities on RO/NF mass transfer, a pilot study, Water Res., 39 (2005) 1233–1244.
[109] B. Van der Bruggen, C. Van de casteele, Modelling of the retention of uncharged molecules with nanofiltration, Water Res., 36 (2002) 1360–1368.
[110] F.F. Chang, W.J. Liu, X.M. Wang, Comparison of polyamide nanofiltration and low-pressure reverse osmosis membranes on As(III) rejection under various operational conditions, Desalination, 334 (2014) 10–16.
[111] S. Déon, B. Lam, P. Fievet, Application of a new dynamic transport model to predict the evolution of performances throughout the nanofiltration of single salt solutions in concentration and diafiltration modes, Water Res., 136 (2018) 22–33.
[112] N. Hilal, H. A1-Zoubi, N.A. Darwish, A.W. Mohammad, M. Abu Arabi, A comprehensive review of nanofiltration membranes: treatment, pretreatment, modelling, and atomic force microscopy, Desalination, 170 (2004) 281–308.
[113] Y. Roy, M.H. Sharqawy, J.H.V. Lienhard, Modeling of flat-sheet and spiral-wound nanofiltration configurations and its application in seawater nanofiltration, J. Membr. Sci., 493 (2015) 630–642.
[114] V. Silva, V. Geraldes, A.M. Brites Alves, L. Palacio, P. Prádanos, A. Hernández, Multi-ionic nanofiltration of highly concentrated salt mixtures in the seawater range, Desalination, 277 (2011) 29–39.
[115] V. Hoshyargar, F. Fadaei, S.N. Ashrafizadeh, Mass transfer simulation of nanofiltration membranes for electrolyte solutions through generalized Maxwell–Stefan approach, Korean J. Chem. Eng., 32 (2015) 1388–1404.
[116] A.R. Hassan, N. Ali, N. Abdull, A.F. Ismail, A theoretical approach on membrane characterization: the deduction of fine structural details of asymmetric nanofiltration membranes, Desalination, 206 (2007) 107–126.
[117] M.A. Al-Obaidi, I.M. Mujtaba, Steady state and dynamic modeling of spiral wound waste water reverse osmosis process, Comput. Chem. Eng., 90 (2016) 278–299.
[118] Y. Garba, S. Taha, N. Gondrexon, G. Dorange, Ion transport modelling through nanofiltration membranes, J. Membr. Sci., 160 (1999) 187–200.
[119] P. Vandezande, L.E.M. Gevers, I.F.J. Vankelecom, Solvent resistant nanofiltration: separating on a molecular level, Chem. Soc. Rev., 37 (2008) 365–405.